CHAPTER - 4

SINGLE NUCLEON TRANSFER REACTIONS

There exists a wide class of nuclear excitations that includes the Gamow-Teller excitations, beta decay, gamma transitions, electromagnetic (M1,E2,M3,E4) transitions, one, two or three nucleon transfer reactions, etc., which can be studied in different ways. Among the nucleon transfer processes, the single nucleon transfer (SNT) reactions are extensively studied, as they give direct information regarding single particle behaviour inside the nucleus through neutron and proton pickup and stripping reactions.

Single particle information as available experimentally from SNT reactions is of considerable interest. The single particle orbits (SPO) and single particle energies (SPE) are the main concepts on any model based on independent particle approximation. Particularly, the nuclear shell model with its spherically symmetric potential gives rise to a set of single particle orbits and corresponding SPEs; the self-consistent Hartree-Fock theory is also based on the existence of such orbits. In the atomic shell model, a major part of the interaction corresponds to the coloumb attraction of electrons by the nucleus, leaving a small part (residual interactions between electrons themselves) which can be treated perturbatively. However, in the nuclear shell model, due to absence of a domineering centre and due to the strong nature of the two-body interaction, the residual nucleon-nucleon interaction cannot be treated perturbatively. This results into large configuration mixing for the description of nuclear states, leading to smearing out of the underlying single particle picture, and thereby spreading a single particle state over a wide energy interval. Inspite of large configuration mixing, the

single particle aspects of many particle wave function help us in understanding the structure and dynamics of nuclei. Many of the measured properties of nuclear states are expectation values of one-body operators in the ground state of the nucleus. For example, the orbit occupancies (which are measured via single nucleon transfer reactions) are the expectation values of the number operator. They have been studied quite extensively using SDM /4,22/. The single particle occupancies are simplest of the dynamical variables in the ground state of the nucleus. These are directly calculable via stripping and pickup sum-rules. Occupanices of excited states are of interest too, as they enter in studies related to compound nucleus formation and are important parameters in the combinatorial theory of level densities.

In this work, we go beyond the occupancies to calculate further single particle aspects, namely the centroid and width of the SNT strength function. These numbers are of vital interest to experimentalists, as they provide information about the excitation energy in the final nucleus upto which an experiment must be conducted so as to exhaust most of the strength. In the absence of configuration mixing, the entire strength could be expected to lie in a single state. This does not happen as there usually is some configuration mixing, and the strength spreads over neighbouring energy states. In that case, one has to take into account the "centre of gravity" of the strength, which can be compared with the theoretical estimate of the centroid of the strength function. The spread of the strength around the centre of a particular single particle state can be measured as 'width' of the strength function, which allows one to estimate the portion of the total strength that has been accounted for in a particular SNT reaction. Though experimental estimate of the width of an SNT reaction has not been evaluated

so far, it is worthwhile calculating these values, and analysing their behaviour in any particular region of interest.

The spectral distribution methods (SDM) developed by French and co-workers /2,3/ are best suited for such calculations as one can make use of major simplicities offered by these methods. Here, one does not require explicit construction of target-state wave function, as is required by the conventional shell model procedure. Single particle properties of our interest namely the occupancies, centroids and widths of the strength function, that are expressed as sum-rule quantities can be written down in terms of traces of powers of H and other operators, which can be calculated without the knowledge of the initial or the final state eigenfunctions.

Any sum-rule quantity is the local expectation value of an operator K with respect to hamiltonian eigenstates, in a chosen space. This can be expanded as a series involving orthogonal polynomials defined on the corresponding eigenstate density. The accuracy of such a calculation depends upon the number of terms used in the expansion. Under the action of the central limit theorem (CLT), only terms upto linear in energy need to be calculated in the series. Polynomial expansion is therefore a handy technique which offers an effective way of dealing with the sum-rule quantities. The operator K could be either the hamiltonian or the number operator, or a product of two or more operators. There is another approach one could follow. If the strength function is assumed to have a definite form like a bivariate gaussian (which it is known to acquire in the CLT limit) /4/, it can be directly integrated to give moments, leading to the sum-rule quantities namely the centroid and width of the strength function.

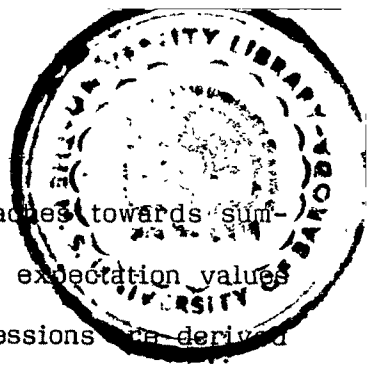

In the next section, we develop these two different approaches towards sum-rule evaluation. Section A gives a detailed theory for the expectation values of operators in terms of a polynomial expansion. All expressions are derived in the configuration space. An approximation for the strength is also given in terms of bivariate gaussian density function, and expressions for centroid and width of the strength function have been obtained in the CLT limit. Calculations have been performed for various nuclei lying in the s-d, f-p and upper f-p-g shells. Results are given in Section B, followed by discussion.

A Theory

A nuclear excitation can be described as the action of an excitation operator O which induces transitions from an initial state $|E\rangle$ to a final state $|E'\rangle$. One then defines a microscopic strength function between $|E\rangle$ and $|E'\rangle$,

$$R(E,E') = |\langle E'|O|E\rangle|^2 \qquad (1)$$

this being the square of the expansion coefficient of the state $O|E\rangle$ in terms of the hamiltonian eigenstates in the final state space. In principle, $R(E,E')$ carries the entire information regarding the transition, and can be used to obtain most of the characteristics of the excitation operator. To begin with, one can obtain energy weighted moments $M^p(E)$ of the strength function

$$M^p(E) = \sum_{E'} R(E,E') \ (E')^p \qquad (2)$$

which gives rise to a variety of sum-rules. Consider a particle transfer to and from a single particle state labelled by s, with an m-particle target

state at energy E. The final state will then be reached in m±1 particle space at energy E'. The excitation operator for particle removal (-) is the destruction operator B_s, the corresponding operator for particle addition being $A_s = B_s^+$. The strength $R_s^-(E,E')$ for particle removal is given by

$$R_s^-(E,E') = |\langle m-1,E'|B_s|m,E\rangle|^2 \tag{3}$$

where $|m,E\rangle$ and $|m-1,E'\rangle$ are respectively the target state and the final state reached as a result of excitation by the operator B_s; both states being the eigenstates of the (1+2)-body hamiltonian in m and (m-1) particle spaces respectively. We shall henceforth drop the indices m and (m-1) whenever that does not cause any confusion. As we are primarily interested in sum-rules, (obtained by appropriately summing up over all final states) we define moments of the strength function $M_s^p(E)$ by:

$$\begin{aligned} M_s^p(E) &= [1/D(m-1)] \sum_{E'} \langle E|A_s|E'\rangle\ (E')^p\ \langle E'|B_s|E\rangle \\ &= [1/D(m-1)] \sum_{E'} \langle E|A_s|E'\rangle\ \langle E'|H^p B_s|E\rangle = \langle E|A_s H^p B_s|E\rangle^m \\ &= \int R_s(E,E')\ (E')^p \rho^{m-1}(E)dE' \qquad (4) \\ &= \{A_s H^p B_s\}^m(E) \end{aligned}$$

where $\rho^m(E)$ is the normalized state density at E in m-particle space, D(m) being the dimensionality or total number of states in m-particle space. In order to write down orthogonal expansion for continuous as well as discrete density of states in the product nucleus space, the summation can be replaced

by integration with a proper weight factor given by the (m-1)-particle density of states at E', which is written as $\rho^{m-1}(E')$ in case of the particle removal strength. $\{O\}^m(E)$ in the above equation is the local expectation value of the operator O at energy E in m-particle space. It is known /29/ that the local expectation value of an arbitrary operator K with respect to the eigenstate $|E\rangle$ can be expressed in the form of a series involving orthogonal polynomials in E defined with respect to the weight function $\rho^m(E)$:

$$\langle E|K|E\rangle = K(E) = \sum_{\mu} \langle K\ P_{\mu}^m(H)\rangle^m\ P_{\mu}^m(E) \qquad (5)$$

where $P_{\mu}^m(E)$ is the μ-th order orthogonal polynomial defined on the m-particle density $\rho^m(E)$. If $\rho^m(E)$ is a gaussian, then the polynomials are Hermite polynomials. The expansion is formally exact, but in practice we truncate the polynomial expansion, which is equivalent to a statistical smoothing operation. This amounts to replacing K(E) by its fluctuation-free form, as higher order terms correspond to fluctuations. In practice, convergence is very rapid as guaranteed by the central limit theorem, for spaces of large number of particles. As a consequence, expectation value K(E), and sum-rule quantities $M^p(E)$ in the central region of the spectra are linear in energy. The linearity of the low-order sum-rule quantities in particular often extends over the entire spectra, and therefore also to the ground state region. If H has eigenvalues E_i, then $H + \alpha K$ with small value of α has the eigenvalues $E_i + \alpha K(E_i)$. If both the spectra are gaussian, this implies merely a scale change in the eigenvalues due to the action of CLT, meaning that $K(E_i)$ is linear in E_i. Hence for the expectation value K(E)

we have

$$K(E) \xrightarrow{CLT} \langle K\rangle^m + \langle K\,(H-E)\rangle^m \left(\frac{W-E}{\sigma^2}\right). \qquad (6)$$

The higher order terms provide corrections to the linear theory. With K = O^+H^pO, this becomes a polynomial expansion for moments of strength function. Replacing K by O^+H^pO, we have for the sum-rule quantities /30,31/,

$$M_s^p(E) = \langle A_sH^pB_s\rangle^m + \langle A_sH^pB_s\hat{H}\rangle^m\,[(E-G(m))]/\sigma^2(m) + \text{higher order terms}. \qquad (7)$$

Here $\langle O\rangle^m$ is the averaged expectation value of O, averaged over all states in m-particle space, G(m) and σ(m) are the centroid and width of the normalized state density $\rho^m(E)$ and $\hat{H} = H-\langle H\rangle^m$. The superscript p which indicates the p^{th} moment of the strength function can take on integral values starting from zero, giving rise to non-energy weighted, linear-energy weighted and higher order sum-rules for particle removal strength.

The non-energy weighted sum-rule (NEWSR) obtained as $\{O^+O\}^m(E)$ gives the total strength of the corresponding reaction. For particle removal strength starting from target state energy E,

$$M_s^0(E) = \{A_sB_s\}^m(E) = \{n_s\}^m(E) \qquad (8)$$

which is the expectation value of the number operator, giving in this case, the occupancy at energy E for a particle in state s in the m-particle space.

Denoting the s-orbit occupancy by $n_s(E,m)$, the polynomial expansion would be

$$n_s(E,m) = \sum_{\mu} \langle n_s P^m_\mu(H)\rangle^m \; P^m_\mu(E) \; .$$

When CLT is completely effective, only terms with $\mu = 0$ and $\mu = 1$ survive in the above equation, giving the linear expansion for occupancy as:

$$n_s(E,m) \xrightarrow{LT} \langle n_s\rangle^m + \langle n_s \; (H-\epsilon(m)\rangle^m \; (E- G(m)) \; / \sigma^2(m) \; . \qquad (9)$$

n_s being a one-body operator, consists of unitary ranks-0 and 1 parts. $\langle n_s\rangle^m$ = m/N corresponds to the average or rank-0 part of n_s. The inner product of n_s with (H-G(m)) comes from unitary rank-1 part of n_s and the hamiltonian H. H is defined by its (1+2) body form:

$$H = \sum_i G_i n_i - 1/4 \sum_{ijkl} W_{ijkl} \; A_i A_j B_k B_l \qquad (10)$$

where G_i is the external single particle energy for the i^{th} orbit and W_{ijkl} is the antisymmetrized two-body matrix element. Decomposing H into unitary ranks, the rank-1 part of H is given by

$$H^{\nu=1} = \sum_i \lambda_i(m) n_i$$

$$= \sum_i (\lambda^{(1)}_i + \lambda^{(2)}_i(m)) n_i$$

λ_i are the traceless single particle energies defined as

$$\lambda^{(1)}_i = G_i - \sum_j G_j/N \text{ and } \lambda^{(2)}_i(m) = \frac{m-1}{N-2} \; (\sum_j W_{ijij} - 1/N \sum_{ij} W_{ijij}) \qquad (11)$$

If one uses spherical orbit notation, the orbits are indexed by angular momentum j. The single particle orbit then has a degeneracy N = 2j+1. If isospin symmetry is considered, then the single particle orbit has a degeneracy of (2j+1) * 2. The two body matrix elements in the spherical orbit representation are denoted by W^{Γ}_{ijkl}, where Γ denotes J or JT, as is the case. The total traceless single particle energy in JT representation is given by

$$\xi_\alpha(m) = \epsilon_\alpha - 1/N \sum_\beta \epsilon_\beta + \frac{m-1}{N-2} \{ 1/N_\alpha \sum_{\beta,J} [J]\ [T]\ W^{JT}_{\alpha\beta\alpha\beta}\ (1 + \delta_{\alpha\beta}) - 1/N \sum_{\alpha,\beta,J} [J]\ [T]\ W^{JT}_{\alpha\beta\alpha\beta} (1 + \delta_{\alpha\beta}) \} \qquad (12)$$

where α, β denote spherical orbits and [J][T]= (2J+1)(2T+1). The expression for occupancy turns out to be

$$n_s(E,m) = m/N\ (1 + (N-m)/(N-1)\ \xi_s(m)\ [(E-\epsilon(m))/\sigma^2(m)] \qquad (13)$$

which has the same form for spherical as well as non-spherical orbits. At a given energy E, the occupancies vary linearly with single particle energy $\xi_s(m)$, which are a function of particle number m.

The centroid energy in the (m-1)-particle space of the corresponding strength is given as the linear-energy weighted sum-rule or LEWSR (p=1).

$$\bar{\xi}_s(E,m) = M^1_s(E) \ / \ M^0_s(E)$$

Since $M^0_s(E) = n_s(E,m)$, we have

$$n_s(E,m)\ \bar{\xi}_s(E,m) = \langle A_s H B_s \rangle^m + \langle A_s H B_s \hat{H} \rangle^m\ [(E-\epsilon(m))/\sigma^2(m)] \qquad (14)$$

The energy region over which the strength is spread is given in terms of the quadratic-energy weighted sum-rule or QEWSR (p = 2)

$$\sigma_s^-(E) = [M_s^2(E) / M_s^0(E) - (\bar{\epsilon}_s^-(E,m))^2]^{\frac{1}{2}} \qquad (15)$$

Expressions are similar for particle addition strength. The total strength for particle addition is just the hole occupancy given by the expectation value $\{B_s A_s\}^m(E) = \{1-A_s B_s\}^m(E)$. Since the total number of particles and holes must add up to give the total degeneracy of an orbit, the hole occupancy can be calculated once the particle occupancy is known. Expressions for particle addition strength centroid and width can be written down similarly, with A_s and B_s operators interchanged in equations (14) and (15).

Due to large dimensionalities of spectroscopic spaces of interest, the ground state, which is the target state in all SNT reactions, lies too far below the centroid $\bar{\epsilon}(m)$ (in terms of $\sigma(m)$) to expect the linear expansion of expectation value resulting from the CLT, to work well in the ground state region. In order to rectify this situation, one can make use of higher order terms, but a more effective and satisfying procedure is to decompose the space of m-particles into configurations defined by distribution of particles into various spherical orbits. Following this, we have decomposed the m-particle space into proton configurations $\vec{m}_p$ and neutron configurations $\vec{m}_n$, where $\vec{m}_p = [m_{1,p}, m_{2,p}, \text{---}]$ with $m_{\alpha,p}$ indicating the number of protons in a spherical orbit α and $m_p = \sum_\alpha m_{\alpha,p}$ = total number of protons; $\vec{m}_n$ being similarly written with $m_n = \sum_\alpha m_{\alpha,n}$, and the total number of particles $m = m_p + m_n$. With this decomposition, the density function has to be accordingly

decomposed into its corresponding configuration expression. The scalar density of states is given in terms of configuration densities as

$$\rho^{m_p,m_n}(E) = \frac{1}{D(m_p,m_n)} \sum_{\vec{m}_p,\vec{m}_n} \rho^{\vec{m}_p,\vec{m}_n}(E)\, D(\vec{m}_p,\vec{m}_n) \,. \tag{16}$$

In the above equation, $\vec{m}$ defines configuration, $D(m_p,m_n)$ is the dimensionality of states in the scalar space defined by m_p protons and m_n neutrons, while $D(\vec{m}_p,\vec{m}_n)$ is the configuration space dimensionality. The scalar expectation value of any operator O is similarly expressed in terms of configuration space expectation values:

$$\{O\}^{m_p,m_n}(E) = \sum_{\vec{m}_p,\vec{m}_n} \{O\}^{\vec{m}_p,\vec{m}_n}(E) \left[\frac{\rho^{\vec{m}_p,\vec{m}_n}(E)\, D(\vec{m}_p,\vec{m}_n)}{\rho^{m_p,m_n}(E)\, D(m_p,m_n)} \right] . \tag{17}$$

The expression in square bracket in the above equation is the fractional intensity of configuration $(\vec{m}_p,\vec{m}_n)$ at energy E. The configuration density $\rho^{\vec{m}_p,\vec{m}_n}(E)$ for all calculations here is assumed to have a gaussian form, so that at energy E, it is given by

$$\rho^{\vec{m}_p,\vec{m}_n}(E) = \frac{1}{(2\pi\sigma^2(m_p m_n))^{1/2}} \exp\left\{ - \frac{(E-\epsilon(\vec{m}_p,\vec{m}_n))^2}{2(\sigma(\vec{m}_p,\vec{m}_n))^2} \right\} \tag{18}$$

where $\epsilon(\vec{m}_p,\vec{m}_n)$ and $\sigma(\vec{m}_p,\vec{m}_n)$ are respectively the centroid and width for

each configuration $(\vec{m}_p, \vec{m}_n)$. Expressions for these in the spherical orbit representation are /1,3/:

$$\epsilon(\vec{m}_p, \vec{m}_n) = \sum_i m_i \epsilon_i + \sum_{ij} m_i (m_j - \delta_{ij})/(1+\delta_{ij})\ \bar{W}_{ij} \qquad (19)$$

where m_i denotes the number of protons or neutrons in the ith orbit, and

$$\bar{W}_{ij} = \sum_J (2J+1)\ W^J_{ijij}\ .$$

For the configuration width, one has

$$\sigma^2(\vec{m}_p, \vec{m}_n) = \sum_{i,j,k,l} PR_{ijkl}\ \ (2J+1)\ (\tilde{W}^J_{ijkl})^2 \qquad (20)$$

where $\tilde{W}^J_{ijkl} = \{W^J_{ijkl} - \delta_{ij}\,\delta_{kl}(1+\delta_{ij}) \sum_J W^J_{ijij}\} \ /\ [N_i\ (N_j - \delta_{ij})]$

and PR_{ijkl} are the propagators for configuration width given by

$$PR_{ijkl} = \frac{1}{4}\,\frac{m_i(m_j-\delta_{ij})}{N_i(N_j-\delta_{ij})} - \frac{1}{2}\,\frac{m_i(m_j-\delta_{ij})(m_k-\delta_{ik}-\delta_{jk})}{N_i(N_j-\delta_{ij})(N_k-\delta_{ik}-\delta_{jk})}$$

$$+ \frac{1}{4}\,\frac{m_i(m_j-\delta_{ij})(m_k-\delta_{ik}-\delta_{jk})(m_l-\delta_{il}-\delta_{jl}-\delta_{kl})}{N_i(N_j-\delta_{ij})(N_k-\delta_{ik}-\delta_{jk})(N_l-\delta_{il}-\delta_{jl}-\delta_{kl})}\ .$$

Since our interest lies in the ground state region, we need to calculate the ground state energy E_g with respect to which occupancies and other sum-rule quantities are calculated. Given a distribution of energy states, the

Ratcliff procedure is used to obtain a discrete energy spectrum. The distribution function $F(E_p)$ at energy E_p is defined as

$$F(E_p) = \int_{-\infty}^{E_p} \rho(E)\, dE \,. \qquad (21)$$

If $\rho(E)$ is a normalised gaussian density, $F(E_p)$ becomes an error function, and $F(\infty) = 1$. $F(E_p)$ would correspond to the total fraction of states below E_p. This, weighted by the total dimensionality D, would give the total number of states below energy level E_p. For a set of completely non-degenerate states, the ground state energy E_g would be that value at which the cumulative distribution function of energy states multiplied by D has a (0→1) jump. For a continuous distribution, this can be estimated at a value = ½. If the states are degenerate in energy, the degeneracy has to be taken into account. For the ground state energy E_g, one has the equation:

$$D * F(E_g) = D * \int_{-\infty}^{E_g} \rho(E)dE = 1/2 * \text{ground state degeneracy} = 1/2(2J+1) \qquad (22)$$

where J is the angular momentum of the ground state, which has to be known experimentally. The density of states $\rho(E)$ (required for the calculation of ground state energy) in the above equation is given by equation 16. Once the ground state energy is calculated, one can calculate higher energy levels using the Ratcliff procedure. It is known that the gaussian density of states does not take care of fluctuations which are maximum at the ground state. The accuracy of calculations using the Ratcliff procedure depends upon the magnitude of these fluctuations. The scalar space therefore often gives a poor approximation for the ground state energy, unless one considers higher

order correction (involving the third and fourth moments) to the density of states. This correction can be made in the form of an Edgeworth series or a Cornish-Fisher expansion around a gaussian density. Level to level fluctuations then reduce to a certain extent /20,32/.

The accuracy in ground state energy calculations can be improved by decomposing the space into configurations. A major advantage is that in the configuration space, many additional pieces of information come in through configuration centroids and widths; whereas in the scalar space, one has to deal with only one centroid and one width. The ground state, which lies far away from the scalar centroid, would therefore be sensitive to higher moments of the scalar density function. In the configuration space however, it is expected that few low-lying configuration centroids may be nearer to the ground state energy, which carry maximum information. One need not calculate higher moments, since fluctuations are minimum as one goes nearer to the centroid. Configuration partitioning thus proves to be a better approximation for the ground state energy calculation than the scalar space low-moment approximation.

For a nucleus whose low lying states are well defined, meaning that the angular momenta and energies of all states below a higher energy state E_{ex} are properly identified, one can use "high energy correction" to calculate the ground state energy. For most of the stable nuclei, it is always possible to identify all low-spin states lying few MeV above the ground state. The energy E_{ex} of one of the states can be calculated using Ratcliff's procedure (Eq.21). The ground state energy is then obtained by simply substracting out the experimentally known energy gap between E_g and E_{ex}. By doing this,

the accuracy is expected to improve slightly - for two reasons: (i) fluctuations, which are maximum at the ground state, get damped at higher energies, and (ii) more experimental information is incorporated .

Once the ground state energy is calculated, all sum-rule quantities are calculated at $E=E_g$. The occupancies so calculated are referred to as the ground-state occupancies. The strength centroids are also measured with respect to the ground state of the target nucleus.

Though the configuration densities $\rho^{\vec{m}_p,\vec{m}_n}(E)$ may not correspond to the eigenvalue density (since configuration symmetry is not necessarily a good symmetry in the eigenspace of a (1+2)-body hamiltonian), it is still possible to define orthogonal polynomials in configuration space through moments of density $\rho^{\vec{m}_p,\vec{m}_n}(E)$. The expectation value of an operator K can be expressed as a polynomial expansion in the configuration space; the expansion being similar to the scalar space expansion:

$$K(E) = \sum_{\vec{m}_p,\vec{m}_n} \frac{\rho^{\vec{m}_p,\vec{m}_n}(E)\; D(\vec{m}_p,\vec{m}_n)}{\rho^{m_p,m_n}(E)\cdot D(m_p,m_n)} \sum_{\mu} \langle K\; P_{\mu}^{\vec{m}_p,\vec{m}_n}(H)\rangle^{\vec{m}_p,\vec{m}_n}\; P_{\mu}^{\vec{m}_p,\vec{m}_n}(E). \quad (23)$$

We can now proceed to obtain expressions for actual operators which we shall be dealing with. For occupancy calculation in the proton-neutron configuration space, $K = n_{i,p}$ or $n_{i,n}$. Due to orthogonality properties of P_μ's and the scalar character of $n_{i,p}$ in the p-n configuration space, it follows that in the spherical orbit representation,

$\langle n_{i,p}\, P_\mu(H)\rangle^{\vec{m}_p,\vec{m}_n}$ = number of protons in the ith orbit

$= m_{i,p}$.

Only $\mu = 0$ term survives in the polynomial expansion giving the occupancy as

$$n_i(E) = \sum_{\vec{m}_p,\vec{m}_n} \frac{D(\vec{m}_p,\vec{m}_n)\rho^{\vec{m}_p,\vec{m}_n}(E)\; m_{i,p}}{D(m_p,m_n)\rho^{m_p,m_n}(E)} .$$

The centroid for particle removal strength is expressed (for s-orbit) as:

$$\xi_s^-(E)\, n_s(E) = \sum_{\vec{m}_p,\vec{m}_n} \frac{\{A_sHB_s\}^{\vec{m}_p,\vec{m}_n}(E)\; D(\vec{m}_p,\vec{m}_n)\,\rho^{\vec{m}_p,\vec{m}_n}(E)}{D(m_p,m_n)\,\rho^{m_p,m_n}(E)} \qquad (24)$$

where

$$\{A_sHB_s\}^{\vec{m}_p,\vec{m}_n}(E) = \langle A_sHB_s\rangle^{\vec{m}_p,\vec{m}_n} + \frac{(E-\epsilon(\vec{m}_p,\vec{m}_n))}{\sigma^2(\vec{m}_p,\vec{m}_n)} \langle A_sHB_s\hat{H}\rangle^{\vec{m}_p,\vec{m}_n} ,$$

$$\hat{H} = H - \langle H\rangle .$$

The above expression is the linear expansion for the local expectation value of particle removal centroid in the configuration space. At this stage, we introduce an operator K_s^- defined by

$$K_s^- = A_sHB_s - 1/2\,(n_sH + Hn_s) . \qquad (25)$$

The operator K_s^- is introduced because A_sHB_s is a three-body operator, whose trace is difficult to calculate. However, when A_sHB_s is split up into K_s^- (which can be shown to have maximum body rank two) and simple three

body operators like $1/2\ (n_s H+Hn_s)$, it can be easily treated in the configuration space. Also we have

$$\begin{aligned} K_s^- &= A_s H B_s - 1/2(n_s H+Hn_s) \\ &= \sum_i \{A_s H(i) B_s - 1/2(n_s H(i)+H(i)n_s)\} \\ &= \sum_i 1/2\{A_s[H(i),B_s] + [A_s,H(i)]B_s\} \end{aligned}$$

where H(i) is the i-body part of H. It turns out that the (i+1)-body part of $A_s H(i) B_s$ and the (i+1)-body part of $-1/2\ (n_s H(i)+H(i)n_s)$ exactly cancel one another; reducing the body rank of K_s^- operator by one. The matrix elements of K_s^- operator are given by:

$$K_s^- = \underbrace{-1/2\{n_s H(1) + H(1)n_s\}}_{\text{one body}} \underbrace{- 1/2\{n_s H(2) + H(2)n_s\}}_{\text{two body}} \qquad (26)$$

The hamiltonian required here is given by equation (10). If ϵ_t and W_{ijkl} represent the single particle energy and antisymmetrized two-body matrix element of H respectively, one has

$$\begin{aligned} K_s^- \text{ (1-body part)} &= -1/2\left[n_s\left(\sum_t \epsilon_t n_t\right) + \left(\sum_t \epsilon_t n_t\right) n_s\right] \\ &= -\sum_t \epsilon_t \delta_{st} n_t = -\epsilon_s n_s \end{aligned}$$

For the two body part of K_s^-, we get

$$\begin{aligned} K_s^- \text{ (2-body part)} &= -1/2\left\{-1/4 \sum_{ijkl} \eta_s W_{ijkl} A_i A_j B_k B_l\right) - \tfrac{1}{4}\left(\sum_{ijkl} W_{ijkl}\ A_i A_j B_k B_l\right) n_s\} \\ &= 1/8 \sum_{i,j,k,l} (\delta_{is} + \delta_{js} + \delta_{ks} + \delta_{ls})\ W_{ijkl}\ A_i A_j B_k B_l \qquad (27) \end{aligned}$$

These expressions can be derived by repeated contraction of destruction and creation operators starting from equation (25). The detailed derivation is given in appendix(II-A). Substituting for K_s^- from equation (25) into equation (24), we have

$$\langle A_s H B_s \rangle^{\vec{m}_p,\vec{m}_n} = \langle K_s^- \rangle^{\vec{m}_p,\vec{m}_n} + 1/2\langle n_s H \rangle^{\vec{m}_p,\vec{m}_n} + 1/2\langle Hn_s \rangle^{\vec{m}_p,\vec{m}_n}$$

$$= \langle K_s^- \rangle^{\vec{m}_p,\vec{m}_n} + m_s \epsilon(\vec{m}_p,\vec{m}_n)$$

where m_s = number of particles in the s-th orbit. Also

$$\langle A_s H B_s \hat{H} \rangle^{\vec{m}_p,\vec{m}_n} = \langle K_s^- H \rangle^{\vec{m}_p,\vec{m}_n} + 1/2\, m_s \langle H\hat{H} \rangle^{\vec{m}_p,\vec{m}_n} + 1/2\langle Hn_s \hat{H} \rangle^{\vec{m}_p,\vec{m}_n}$$

These expressions when inserted in the equation (24), yield the final expression for particle removal centroid as

$$\xi_s^-(E)\, n_s(E) = \sum_{\vec{m}_p,\vec{m}_n} \frac{\rho^{\vec{m}_p,\vec{m}_n}(E)\, D(\vec{m}_p,\vec{m}_n)}{\rho^{m_p,m_n}(E)\, D(m_p,m_n)} \Big[\langle K_s^- \rangle^{\vec{m}_p,\vec{m}_n} + m_s \epsilon(\vec{m}_p,\vec{m}_n) + \frac{(E-\epsilon(\vec{m}_p,\vec{m}_n))}{\sigma^2(\vec{m}_p,\vec{m}_n)} \langle K_s^- \hat{H} \rangle^{\vec{m}_p,\vec{m}_n} + 1/2\, m_s \sigma^2(\vec{m}_p,\vec{m}_n) + 1/2\langle Hn_s \hat{H} \rangle^{\vec{m}_p,\vec{m}_n} \Big] \quad (28)$$

One can work out similarly for particle addition strength. For the stripping reaction, we define a Hermitian operator K_s^+ by:

$$K_s^+ = B_s H A_s - 1/2\,(B_s A_s H + H B_s A_s) \quad (29)$$

The expectation value of $B_s H A_s$ divided by the total strength (i.e.

expectation value of $B_s A_s = 1 - n_s(E))$ gives the centroid for particle addition strength. However, K_s^+ is related to K_s^-, and therefore its matrix elements need not be explicitly calculated /31/. From equation (29), we have

$$K_s^+ = 1/2\ B_s\ [H,A_s] + 1/2\ [B_s,H]\ A_s$$
$$= K_s^- + 1/2\{B_s,\ [H,A_s]_-\}_+ - 1/2\{A_s,[H,B_s]_-\}_+ \qquad (30)$$

where the double commutator indicates further reduction of body rank. The final expression for $(K_s^+ - K_s^-)$ contains effective one-body terms:

$$K_s^+ - K_s^- = \epsilon_s + \sum_j W_{sjsj}\ n_j\ . \qquad (31)$$

An explicit derivation of this result is included in the appendix(II-B).

It turns out that the centroids of particle removal strength and particle addition strength are connected through a well known identity /21/

$$\{(\mathcal{E}_s^+(E) - E)\ (2j_s + 1 - n_s(E)) - (\mathcal{E}_s^-(E) - E) n_s(E)\} /\ (2j_s + 1)$$

$$= \epsilon_s + \sum_t n_t(E)\ \{1 - \delta_{st} / (2j_t + 1)\}\ \bar{W}_{st} \qquad (32)$$

where s and t represent spherical orbits for protons and neutrons, j_s is the angular momentum for the s-orbit, ϵ_s is the corresponding single particle energy and $\bar{W}_{st}$ is the average two body matrix element between spherical orbits s and t. This expression appears as a special monopole case of the particle-hole relationship for the general linear energy weighted multipole sum-rules /33/.

Following are the necessary averages for the occupancy and particle removal centroid calculation in configuration linear approximation: $\langle n_s \rangle^{\vec{m}_p, \vec{m}_n}$, $\langle H \rangle^{\vec{m}_p, \vec{m}_n}$ $\langle H^2 \rangle^{\vec{m}_p, \vec{m}_n}$, $\langle A_s H B_s \rangle^{\vec{m}_p, \vec{m}_n}$, $\langle A_s H B_s \hat{H} \rangle^{\vec{m}_p, \vec{m}_n}$, $\langle n_s \hat{H} \rangle^{\vec{m}_p, \vec{m}_n}$ and $\langle H n_s \hat{H} \rangle^{\vec{m}_p, \vec{m}_n}$. Computer programmes for evaluation of these have been developed in spherical orbit p-n formalism; the subscript s then represents a spherical orbit for protons or neutrons with angular momentum j_s.

The width $\bar{6}_s(E)$ calculation for SNT strength in configuration linear approximation requires evaluation of $\langle A_s H^2 B_s \hat{H} \rangle^{\vec{m}_p, \vec{m}_n}$, average of an operator involving the third power of (1+2)-body H. Evaluation of this average involving H^3 is too much time consuming and tedious, due to two reasons: (i) the complexity and number of operations increase rapidly with increase in the power of H and (ii) the number of configurations in the space of interest is also large. Hence, at this stage, it is enough to engender its estimate using a simple approximation indicated by Kota and Kar /4/. Here, we briefly review their arguments.

It turns out the hamiltonian can be written down as a sum of its noninteracting and interacting parts so that H = h + V, where h indicates the noninteracting particle (NIP) hamiltonian and V corresponds to the interacting part. For noninteracting particles, the state density for large m turns out to be gaussian. One examines changes introduced in the NIP picture when V is switched on. With configuration partitioning of space, one has $V = V^{[0]} + V^{[2]}$ where $V^{[0]}$ is the scalar part which gives rise to configuration centroids. $V^{[2]}$ is the tensor component and gives configuration widths and higher moments. Most of the $V^{[0]}$ causes either none, or negligible change in the structure of NIP density. $V^{[2]}$ produces excitations and spreadings within a

subspace, the spread corresponding to configuration widths $\sigma(\vec{m})$, which is nearly constant in a subspace. $V^{[0]}$ itself can be decomposed according to different unitary ranks.

$$V^{[0]} = \sum_{\nu=0}^{2} V^{\nu,[0]} .$$

The (0+1)-rank part of $V^{\nu,[0]}$ is absorbed in h, resulting in a slight centroid shift, but no other specific change. $V^{2,[0]}$ part is neglected as it turns out to be small. It is well established that different unitary ranks of the hamiltonian propagate independently, and their probability densities can be convoluted. Under the approximation of constant configuration width, the intensity function can be expressed as a convolution of NIP intensity with an interaction gaussian:

$$I^{m}(E) = \sum_{\vec{m}} I^{\vec{m}}(E) = \sum_{\vec{m}} I^{\vec{m}}_{NIP}(E) \otimes \rho^{\vec{m}}_{G}(E) . \qquad (33)$$

Arguments can be extended to strength function R(E,E'). The density weighted strength function $S(E,E')=d(m')\rho^{m'}(E')|\langle m',E'|O|E,m\rangle|^{2}d(m)\rho^{m}(E)/\langle\langle O^{+}O\rangle\rangle^{m}$ for an excitation operator O can be seen to be bivariate density function, which, under CLT, acquire a bivariate density form/4,34/

$$S(E,E') \xrightarrow{CLT} S_{G}(E,E') .$$

The strength intensity for non-interacting hamiltonian may be denoted by $I_{h}(E,E')$. The final structure of the intensity when the interaction is switched on is similar to a bivariate gaussian in the CLT limit. One heuristically assumes that the strength follows the densities, so that the spread around the configuration centroids when interaction V is switched on is assumed to be a bivariate gaussian. The strength intensity for the total hamiltonian is

$$I_H(E,E') = \langle\langle O^+O\rangle\rangle^m S(E,E') = I_h \otimes S_G^V (E,E')$$
$$= \iint I_h(x,y)\, S_G^V (E-x,E'-y)\, dxdy\,. \qquad (34)$$

For NIP intensity, one has

$$I_h(x,y) = \sum_{\vec{m},\vec{m}'} |\langle \vec{m}'|O|\vec{m}\rangle|^2\, d(\vec{m})d(\vec{m}')\, \delta(x-\epsilon(\vec{m}))\, \delta(y-\epsilon(\vec{m}')) \qquad (35)$$

Substituting in the above equation, one finally obtains

$$I_H(E,E') = \sum_{\vec{m},\vec{m}'} |\langle \vec{m}'|O|\vec{m}\rangle|^2\, d(\vec{m})d(\vec{m}')\, S_G^V((E-\epsilon(\vec{m}))\,(E'-\epsilon(\vec{m}'))) \qquad (36)$$

Under further p-n partitioning of space, for better results near the ground state, it can be seen that in the space of (m_p,m_n), the strength function (without density weights) is given by:

$$R(E,E') = |\langle E'|O|E\rangle|^2 = \sum_{\substack{\vec{m}_p,\vec{m}_n \\ \vec{m}_p',\vec{m}_n'}} \frac{I^{\vec{m}_p,\vec{m}_n}(E) I^{\vec{m}_p',\vec{m}_n'}(E')}{I^{m_p,m_n}(E) I^{m_p',m_n'}(E')} |\langle \vec{m}_p,\vec{m}_n|O|\vec{m}_p',\vec{m}_n'\rangle|^2 \qquad (37)$$

$$* \frac{S_G(E,E',\epsilon(\vec{m}_p,\vec{m}_n),\epsilon(\vec{m}_p',\vec{m}_n'),\sigma(\vec{m}_p,\vec{m}_n),\sigma(\vec{m}_p',\vec{m}_n'),\zeta_2)}{\rho^{\vec{m}_p,\vec{m}_n}(E)\,\rho^{\vec{m}_p',\vec{m}_n'}(E')}$$

with $I(E)$ = dimensionality $* \rho(E) = d(m)\,\rho(E)$,

$$|\langle \vec{m}_p,\vec{m}_n|O|\vec{m}_p',\vec{m}_n'\rangle|^2 = \sum_{\substack{\alpha \in \vec{m}_p,\vec{m}_n \\ \beta \in \vec{m}_p',\vec{m}_n'}} |\langle \vec{m}_p',\vec{m}_n',\beta|O|\vec{m}_p,\vec{m}_n,\alpha\rangle|^2 * [D(\vec{m}_p,\vec{m}_n)\, D(\vec{m}_p',\vec{m}_n')]^{-1}$$

$$\text{and } \zeta_2 = \langle O^\dagger H^{\nu=2}\ O\ H^{\nu=2}\rangle^{m_p,m_n} / \langle O^\dagger O\rangle^{m_p,m_n}\langle H^{\nu=2}\ H^{\nu=2}\rangle^{m_p,m_n} \quad (38)$$

S_G in the above equation is a bivariate gaussian density function at E and E' parametrized by two configuration centroids $\epsilon(\vec{m}_p,\vec{m}_n)$, $\epsilon(\vec{m}_p',\vec{m}_n')$, two configurations widths $\sigma(\vec{m}_p,\vec{m}_n)$, $\sigma(\vec{m}_p',\vec{m}_n')$ and by a correlation coefficient ζ_2 in the space of m_p protons and m_n neutrons. $H^{\nu=2}$ in the above equation is the irreducible rank-2 part of H, when H is decomposed according to irreducible parts with respect to the group $U(N/2)_p + U(N/2)_n$, where the proton and neutron oribts have been differentiated with; N/2 being the total number of single particle states for either protons or neutrons. The primed configurations are the ones reached in the final nucleus as a result of excitation from a state in unprimed configuration in the target state. Thus the density weighted strength function is seen to be a superposition of bivariate gaussian forms, and hence can be easily used to evaluate its various moments, by integrating with respect to E'.

It must be noted that the correlation coefficient ζ_2 that is used in the above equation is calculated in the p-n scalar space, and not in the configuration space. The traces needed to evaluate ζ_2 in particle removal space(with $O \equiv B_S$)are $\langle A_S H^{\nu=2} B_S H^{\nu=2}\rangle^{m_p,m_n}$, $\langle A_S B_S\rangle^{m_p,m_n}$ and scalar width $\langle H^{\nu=2} H^{\nu=2}\rangle^{m_p,m_n}$. One can simplify further by writing

$$A_S H^{\nu=2} B_S H^{\nu=2} = (K_S^- + 1/2(n_S H^{\nu=2} + H^{\nu=2} n_S)) H^{\nu=2}, \text{ so that}$$

$$\zeta_2 = \frac{\langle K_S H^{\nu=2}\rangle^{m_p,m_n} + 1/2\ m_s\sigma^2(m_p,m_n) + 1/2\langle H^{\nu=2} n_S H^{\nu=2}\rangle^{m_p,m_n}}{m_s\sigma^2(m_p,m_n)} \quad (39)$$

The occupancy weighted centroid of the particle removal strength in terms of moments of the strength density function turns out to be

$$\bar{\mathcal{E}}_s^-(E)n_s(E) = \sum_{\substack{\vec{m}_p,\vec{m}_n,\\ \vec{m}_p',\vec{m}_n'}} \rho^{\vec{m}_p,\vec{m}_n}(E)\ m_s\{\epsilon(\vec{m}_p',\vec{m}_n') + \zeta_2(E-\epsilon(\vec{m}_p,\vec{m}_n)) * \sigma(\vec{m}_p',\vec{m}_n')/\sigma(\vec{m}_p,\vec{m}_n)\} \quad (40)$$

while the second moment of particle removal strength is

$$W_s^-(E)n_s(E) = \sum_{\substack{\vec{m}_p,\vec{m}_n\\ \vec{m}_p',\vec{m}_n'}} \rho^{\vec{m}_p,\vec{m}_n}(E)\ m_s[\left\{\epsilon(\vec{m}_p',\vec{m}_n') + \frac{\zeta_2(E-\epsilon(\vec{m}_p,\vec{m}_n)) * \sigma(\vec{m}_p',\vec{m}_n')}{\sigma(\vec{m}_p,\vec{m}_n)}\right\}^2 + \sigma^2(\vec{m}_p',\vec{m}_n')\ (1-\zeta_2^2)] . \quad (41)$$

The width of particle removal strength would simply be

$$\sigma_s^-(E) = [W_s^-(E) - (\bar{\mathcal{E}}_s^-(E))^2]^{\frac{1}{2}} . \quad (42)$$

All the necessary averages (as indicated earlier) when the excitation operator O is a particle removal operator B_s and particle addition operator A_s have been calculated and used for evaluation of particle removal and addition centroids and widths with respect to the energy of the target nucleus. We have thus calculated $\bar{\mathcal{E}}_s^-(E)$ in two different ways; (i) by using the standard configuration linear expression for linear energy weighted sum-rule and (ii) by exploiting the bivariate normal form of the density weighted strength function. The width estimate for particle removal and addition strengths is based only on the bivariate density form.

B Results and Discussion

(a) sd shell

As mentioned earlier, out of the many effective interactions designed for use in 2s-1d shell, only two of them have been shown to agree /17,23/, within reasonable error limits, with the experimental results of $s_{1/2}$ orbit occupancy. The PW interaction /35/ is derived from Kuo-Brown interaction by adjusting certain two-body matrix elements to obtain a good fit to the levels of A=18 to 22 nuclei and to give better predictions for excited rotational bands in these nuclei. The universal s-d interaction /36/ has been similarly obtained but in addition has the two-body matrix elements with a mild dependence on total number of nucleons in the nucleus. The calculation of necessary averages in case of the universal s-d interaction is a bit more troublesome, as one has to start from square one for each new nucleus because of the number dependence of two-body matrix elements. The PW interaction employs the ^{17}O levels as the external single particle energy levels (-4.15, -3.28 and 0.93 MeV for $d_{5/2}$, $s_{1/2}$ and $d_{3/2}$ orbits respectively) and the corresponding single particle energies for the universal s-d interaction are (-3.95, -3.18 and 1.65 MeV respectively). Earlier, calculations for occupancies in 2s-1d shell using these two interactions have been performed in m,T (Configuration-Isospin) formalism; while in this work, the space is decomposed according to proton-neutron configurations, so that one can talk directly about proton or neutron transfers.

Table 4.1 gives the orbit occupancies for various nuclei in the 2s-1d shell alongwith the experimental values from /17/ and /37/. Table 4.2 gives the particle transfer centroids and widths for several nuclei. For each nucleus

in Table-4.2a/b, columns 1 to 6 respectively give the following quantities:

1 proton/neutron removal centroid calculated using polynomial expansion upto the linear term in configuration space;

2 proton/neutron removal centroid with the assumption of bivariate gaussian strength function;

3 proton/neutron removal width;

4 proton/neutron addition centroid† using polynomial expansion method;

5 proton/neutron addition centroid† using bivariate gaussian strength function, and

6 proton/neutron addition width.

Sub-columns for two interactions are labelled appropriately. For nuclei with equal number of protons and neutrons, both the proton and neutron transfer results are identical due to the proton-neutron symmetric nature of the effective interactions. All the results are in MeV and are with reference to the ground state energy of the target nucleus. The ground state energies are calculated using the Ratcliff procedure /16/ with excited-state correction whenever the identification of all excited states upto a certain energy is complete. These calculated ground-state energies for few nuclei are given in Table 4.3 for completeness of information. Table 4.3 gives the values of occupancy dependent single particle energy as defined in equation 32. The first row for each nucleus corresponds to values obtained using the universal s-d interaction, while the PW interaction results are given in the second row. Table-4.4 gives the coulomb corrected values of occupany dependent single particle energies for protons and the experimental values are taken from a recent paper by Ishkhanov et al /37/.

† Values exceeding 100 MeV are replaced by the figure 100.

Table 4.1: Ground-state proton and neutron occupancies for s-d shell nuclei

Nucl	Int	Proton occupancy			Neutron occupancy		
		d5/2	s1/2	d3/2	d5/2	s1/2	d3/2
	U	1.79	0.20	0.01	1.79	0.20	0.01
20	PW	1.81	0.17	0.02	1.81	0.17	0.02
Ne	R8	1.20	0.40	0.40			
	R5	1.10	0.50	0.30	1.10	0.20	0.70
	U	1.78	0.18	0.04	2.73	0.24	0.03
21	PW	1.79	0.15	0.06	2.72	0.23	0.05
Ne	R8						
	R5		0.80			1.10	
	U	1.76	0.18	0.06	3.66	0.31	0.04
22	PW	1.77	0.15	0.08	3.61	0.33	0.06
Ne	R8	1.30	0.65	0.05			
	R5	1.30	0.50	0.10		0.30	
	U	2.73	0.24	0.03	1.78	0.18	0.04
21	PW	2.74	0.22	0.04	1.80	0.15	0.05
Na	R8						
	R5						
	U	2.64	0.26	0.10	3.56	0.35	0.09
23	PW	2.65	0.23	0.12	3.52	0.35	0.13
Na	R8	2.90	0.10	0.00			
	R5		0.25			0.30	
	U	3.57	0.33	0.10	3.57	0.33	0.10
24	PW	3.52	0.33	0.15	3.52	0.33	0.15
Mg	R8	3.20	0.30	0.50			
	R5	3.13	0.50	0.53	3.25	0.25	0.50
	U	3.46	0.37	0.17	4.30	0.51	0.19
25	PW	3.48	0.32	0.20	4.26	0.50	0.24
Mg	R8						
	R5	3.20	0.50	0.30			
	U	3.49	0.34	0.17	5.09	0.70	0.21
26	PW	3.53	0.28	0.19	4.96	0.73	0.30
Mg	R8	3.30	0.50	0.30			
	R5	3.28	0.47	0.25	5.10	0.37	0.57
	U	4.32	0.50	0.18	3.47	0.36	0.17
25	PW	4.27	0.49	0.23	3.49	0.32	0.19
Al	R8						
	R5						
	U	4.24	0.51	0.25	4.24	0.51	0.25
26	PW	4.24	0.48	0.28	4.24	0.48	0.28
Al	R8						

Table 4.1: Contd....

Nucl	Int	Proton occupancy			Neutron occupancy		
		d5/2	s1/2	d3/2	d5/2	s1/2	d3/2
	U	4.26	0.49	0.25	4.96	0.71	0.32
27	PW	4.30	0.43	0.27	4.94	0.69	0.38
Al	R8	4.80	0.20	0.0			
	R5		0.1			0.6	
	U	4.32	0.45	0.23	5.47	1.04	0.49
28	PW	4.40	0.38	0.22	5.41	1.03	0.56
Al	R8						
	R5						
	U	5.04	0.66	0.29	5.04	0.66	0.29
28	PW	5.05	0.61	0.34	5.05	0.61	0.34
Si	R8	4.50	0.75	0.75			
	R5	4.50	0.45	0.63	5.10	0.73	0.30
	U	4.97	0.68	0.35	5.40	1.01	0.59
29	PW	5.05	0.60	0.35	5.48	1.00	0.62
Si	R8						
	R5				5.30	1.10	0.60
	U	5.11	0.62	0.27	5.69	1.37	0.94
30	PW	5.20	0.54	0.26	5.70	1.37	0.93
Si	R8	4.80	0.60	0.60			
	R5	5.38	0.40	0.25	5.67	0.90	1.37
	U	5.42	1.01	0.57	4.99	0.67	0.34
29	PW	5.42	0.97	0.61	5.07	0.59	0.34
P	R8						
	R5						
	U	5.43	1.00	0.57	5.43	1.00	0.57
30	PW	5.49	0.94	0.57	5.49	0.94	0.57
P	R8						
	R5						
	U	5.59	0.98	0.42	5.74	1.37	0.89
31	PW	5.63	0.93	0.43	5.78	1.39	0.83
P	R8	6.00	1.00	0.00			
	R5		1.10		6.00	1.60	0.50
	U	5.79	1.38	0.83	5.79	1.38	0.83
32	PW	5.82	1.42	0.76	5.82	1.42	0.76
S	R8	5.75	1.45	0.80			
	R5	5.90	1.20	0.90	5.83	1.27	0.90
	U	5.83	1.38	0.79	5.86	1.61	1.53
33	PW	5.88	1.44	0.68	5.90	1.71	1.38
S	R8						
	R5		1.30			1.50	

Table 4.1: Contd...

Nucl	Int	Proton occupancy			Neutron occupancy		
		d5/2	s1/2	d3/2	d5/2	s1/2	d3/2
	U	5.93	1.45	0.62	5.93	1.79	2.27
34	PW	5.97	1.53	0.50	5.96	1.89	2.15
S	R8	5.80	1.70	0.50			
	R5						
	U	5.85	1.61	1.54	5.83	1.37	0.80
33	PW	5.90	1.71	1.39	5.87	1.44	0.69
Cl	R8						
	R5						
	U	5.98	1.73	1.29	5.97	1.84	2.19
35	PW	6.00	1.88	1.13	5.99	1.93	2.07
Cl	R8	6.00	1.85	1.15			
	R5	6.00	1.67	1.33	6.00	1.80	2.20
	U	6.00	1.92	2.08	6.00	1.92	2.08
36	PW	6.00	1.98	2.02	6.00	1.98	2.02
Ar	R8	5.80	1.70	2.30			
	R5	5.90	1.80	2.30	5.75	1.75	2.45

R5: Reference no.17, R8: Reference no.37.

Table 4.2a: Centroids and Widths for proton removal(-) and addition(+) strengths for s-d shell nuclei.

NUCL		EM1		EM2		SIG-		EP1		EP2		SIG+	
		U	PW	U	PW	U	PW	U	PW	U	PW	U	PW
^{20}Ne	d5	18.2	18.0	20.5	20.7	3.4	3.3	-4.4	-4.2	-3.5	-3.0	5.3	5.3
	s1	17.7	17.3	20.5	20.0	3.4	3.3	-4.9	-4.5	-4.6	-4.2	5.3	5.3
	d3	15.6	15.5	18.7	18.7	3.4	3.3	-2.4	-2.2	-2.4	-2.2	5.2	5.4
^{21}Ne	d5	19.4	23.6	20.7	20.8	3.8	3.8	-6.6	-4.4	-6.0	-5.6	5.5	5.6
	s1	18.2	26.4	20.1	19.4	3.9	3.8	-6.4	-5.0	-6.2	-5.6	5.5	5.6
	d3	16.7	77.1	18.3	18.1	3.9	3.8	-4.0	-2.7	-4.0	-3.6	5.5	5.7
^{22}Ne	d5	21.6	21.7	22.4	22.9	4.0	4.1	-8.1	-7.8	-7.8	-7.3	5.5	5.7
	s1	20.5	20.4	21.6	21.1	4.2	4.0	-7.7	-6.8	-7.6	-6.8	5.6	5.6
	d3	19.2	19.3	19.7	20.0	4.1	4.0	-5.6	-5.0	-5.6	-5.0	5.6	5.8
^{21}Na	d5	16.9	22.8	19.8	20.8	4.3	4.4	-2.4	3.1	.1	1.4	5.7	5.8
	s1	14.8	26.5	18.8	19.1	4.4	4.3	-4.8	-2.9	-4.3	-3.8	5.6	5.7
	d3	12.7	168.3	16.8	17.6	4.4	4.3	-2.6	-.6	-2.6	-2.2	5.5	5.7
^{23}Na	d5	20.8	20.9	21.9	22.7	4.7	4.8	-5.7	-5.3	-4.9	-3.9	5.7	5.9
	s1	18.5	18.4	20.3	20.1	4.8	4.7	-7.3	-6.5	-7.1	-6.3	5.8	5.9
	d3	17.0	17.1	15.1	18.6	4.8	4.7	-5.7	-4.9	-5.7	-4.9	5.7	6.0
^{24}Mg	d5	20.8	21.0	22.3	23.3	5.1	5.3	-1.0	-.4	1.2	2.8	5.8	6.1
	s1	17.6	17.7	20.1	20.2	5.2	5.2	-6.9	-5.9	-6.4	-5.4	5.9	6.0
	d3	15.9	16.1	17.6	18.2	5.2	5.2	-5.9	-4.9	-5.8	-4.9	5.7	6.1
^{25}Mg	d5	21.6	21.9	22.1	23.1	5.0	5.2	-4.3	-3.5	-3.6	-1.8	5.6	5.9
	s1	18.5	18.4	19.6	19.7	5.1	5.1	-8.3	-7.3	-8.0	-7.1	5.6	5.8
	d3	16.7	16.9	17.0	17.6	5.1	5.0	-7.2	-6.2	-7.2	-6.1	5.5	5.9
^{26}Mg	d5	23.2	23.7	23.0	24.1	4.7	4.9	-5.5	-4.7	-5.8	-4.0	5.3	5.6
	s1	20.2	20.0	20.4	20.3	4.9	4.8	-9.8	-8.9	-9.7	-8.9	5.3	5.4
	d3	18.5	18.5	17.8	18.3	4.9	4.8	-8.7	-7.6	-8.8	-7.6	5.2	5.5
^{25}Al	d5	19.8	19.9	21.4	22.4	5.4	5.7	4.8	4.8	8.7	10.8	5.9	6.2
	s1	15.9	15.9	18.5	18.8	5.6	5.6	-6.4	-5.2	-5.5	-4.2	5.9	6.1
	d3	13.9	12.5	15.6	16.3	5.6	5.6	-5.9	-4.9	-5.8	-4.7	5.6	6.1
^{26}Al	d5	21.0	21.3	21.5	22.7	5.2	5.5	1.2	1.8	2.5	5.3	5.7	6.0
	s1	17.2	17.1	18.5	18.6	5.4	5.4	-7.7	-6.6	-7.3	-6.1	5.7	5.8
	d3	15.1	15.2	15.5	16.1	5.4	5.4	-7.3	-6.0	-7.3	-6.0	5.4	5.9
^{27}Al	d5	22.5	23.0	22.3	23.6	4.9	5.2	-.2	1.1	-.8	2.6	5.4	5.7
	s1	18.6	18.5	18.9	19.1	5.1	5.1	-9.3	-8.3	-9.2	-8.1	5.3	5.5
	d3	16.6	16.7	15.9	16.6	5.1	5.0	-8.8	-7.4	-8.8	-7.4	5.1	5.5
^{28}Al	d5	23.9	24.6	22.9	24.3	4.5	4.8	-.9	1.2	-3.5	.5	4.9	5.3
	s1	19.9	19.6	19.3	19.4	4.7	4.7	-11.1	-10.3	-11.3	-10.3	4.9	5.0
	d3	18.0	17.9	16.3	16.8	4.7	4.6	-10.2	-8.7	-10.3	-8.8	4.7	5.0

Table 4.2a: Contd.....

NUCL		EM1		EM2		SIG-		EP1		EP2		SIG+	
		U	PW	U	PW	U	PW	U	PW	U	PW	U	PW
^{28}Si	d5	22.3	22.7	22.1	23.5	5.1	5.4	15.5	16.5	14.7	20.9	5.3	5.7
	s1	17.6	17.7	18.2	18.5	5.3	5.3	-8.4	-7.2	-8.2	-6.8	5.3	5.5
	d3	15.3	15.7	14.7	15.5	5.3	5.2	-8.9	-7.4	-9.0	-7.5	5.0	5.4
^{29}Si	d5	23.2	23.8	22.1	23.7	4.6	5.0	9.2	13.5	4.2	13.0	4.8	5.2
	s1	18.5	18.4	18.0	18.2	4.8	4.9	-10.3	-9.4	-10.6	-9.4	4.8	5.0
	d3	16.2	16.2	14.6	15.1	4.8	4.8	-10.2	-8.5	-10.3	-8.6	4.5	4.9
^{30}Si	d5	24.6	25.3	22.8	24.4	4.1	4.5	13.2	19.9	2.5	13.7	4.3	4.7
	s1	19.8	19.3	18.4	18.4	4.2	4.4	-12.3	-11.7	-12.9	-12.0	4.2	4.4
	d3	17.6	17.0	14.8	14.9	4.2	4.2	-11.6	-9.7	-11.8	-9.9	3.9	4.3
^{29}P	d5	21.3	21.5	21.1	22.5	5.2	5.6	29.7	29.5	28.0	38.5	5.1	5.6
	s1	16.2	16.1	16.8	17.0	5.4	5.4	-7.1	-5.4	-6.5	-4.6	5.1	5.3
	d3	13.7	13.9	13.1	13.5	5.3	5.3	-8.7	-6.9	-8.8	-7.0	4.8	5.3
^{30}P	d5	22.5	23.0	21.5	23.1	4.7	5.2	28.2	33.6	18.5	34.5	4.7	5.1
	s1	17.4	17.3	17.0	17.2	4.9	5.0	-9.1	-7.8	-9.5	-7.8	4.7	4.9
	d3	14.9	14.7	13.3	13.5	4.9	4.8	-10.1	-8.1	-10.4	-8.4	4.4	4.7
^{31}P	d5	24.1	24.8	22.3	24.1	4.2	4.6	50.7	61.4	25.0	49.3	4.1	4.6
	s1	18.8	18.5	17.5	17.6	4.3	4.5	-10.9	-10.3	-12.2	-11.1	4.1	4.4
	d3	16.3	15.7	13.4	13.5	4.3	4.3	-11.5	-9.4	-11.9	-9.7	3.8	4.1
^{32}S	d5	23.1	22.9	21.2	23.0	4.1	4.7	86.5	100.0	36.7	88.9	3.8	4.3
	s1	17.8	17.6	16.5	16.8	4.4	4.5	-8.9	-7.3	-11.8	-9.1	3.8	4.2
	d3	15.1	14.2	12.3	11.9	4.2	4.2	-11.3	-8.8	-12.0	-9.4	3.6	3.8
^{33}S	d5	24.1	24.9	21.5	23.6	3.4	4.0	100.0	100.0	14.9	95.7	3.1	3.6
	s1	18.8	18.4	16.7	17.0	3.7	3.9	-11.1	-10.1	-15.7	-13.7	3.1	3.5
	d3	16.1	14.7	12.3	11.4	3.4	3.4	-12.6	-9.8	-13.6	-10.5	2.8	3.1
^{34}S	d5	25.4	26.3	22.2	24.5	2.7	3.2	100.0	100.0	8.0	100.0	2.4	2.5
	s1	19.8	19.2	17.1	17.4	3.0	3.2	-12.3	-11.6	-19.2	-17.2	2.4	2.6
	d3	17.0	15.2	12.2	10.9	2.6	2.4	-14.1	-10.9	-14.9	-11.6	2.1	2.1
^{33}Cl	d5	21.8	22.3	20.0	21.9	4.1	4.7	86.8	100.0	12.6	100.0	3.4	4.0
	s1	17.0	16.6	15.7	16.0	4.2	4.4	-7.6	-3.5	-12.9	-7.1	3.5	3.9
	d3	14.2	12.7	11.5	10.5	4.0	4.0	-10.9	-7.9	-12.6	-9.1	3.2	3.5
^{35}Cl	d5	24.4	25.4	21.2	23.7	2.5	3.2	100.0	100.0	100.0	100.0	2.0	2.5
	s1	19.1	18.6	16.5	16.8	2.9	3.0	-9.7	-2.3	-27.0	-29.3	2.1	2.3
	d3	16.4	14.1	11.6	9.8	2.3	2.0	-13.7	-10.0	-16.0	-11.7	1.7	1.6
^{36}Ar	d5	23.6	24.6	20.2	22.9	2.4	3.2	100.0	100.0	100.0	100.0	1.6	6.0
	s1	18.6	18.0	15.9	15.8	2.8	2.8	-3.3	46.1	-70.7	2.8	1.8	2.0
	d3	16.2	13.2	11.0	8.0	2.0	1.3	-12.9	-8.3	-18.6	1.3	1.3	2.0

Table 4.2b: Centroids and widths for neutron removal(-) and addition(+) strengths for s-d shell nuclei.

NUCL		EM1		EM2		SIG-		EP1		EP2		SIG+	
		U	PW	U	PW	U	PW	U	PW	U	PW	U	PW
^{20}Ne	d5	18.2	18.0	20.5	20.7	3.4	3.3	-4.4	-4.2	-3.5	-3.0	5.3	5.3
	s1	17.7	17.3	20.5	20.0	3.4	3.3	-4.9	-4.5	-4.6	-4.2	5.3	5.3
	d3	15.6	15.5	18.7	18.7	3.4	3.3	-2.4	-2.2	-2.4	-2.2	5.2	5.4
^{21}Ne	d5	16.9	21.9	19.8	20.0	4.3	4.4	-2.4	2.2	.1	.6	5.7	5.8
	s1	14.8	24.9	18.8	18.4	4.4	4.3	-4.8	-3.0	-4.3	-3.8	5.6	5.8
	d3	12.7	13.5	16.8	16.7	4.4	4.3	-2.6	-.7	-2.6	-2.1	5.5	5.7
^{22}Ne	d5	17.0	17.0	20.8	21.4	5.0	5.1	2.7	3.0	8.5	9.6	5.9	6.1
	s1	13.9	13.7	19.0	19.2	5.0	5.0	-4.5	-3.9	-3.6	-2.8	5.8	6.0
	d3	11.7	11.7	16.8	17.2	5.0	5.0	-2.8	-2.2	-2.8	-2.2	5.6	5.9
^{21}Na	d5	19.4	24.5	20.7	21.5	3.8	3.8	-6.6	-4.0	-6.0	-5.3	5.5	5.6
	s1	18.2	27.7	20.1	20.1	3.9	3.8	-6.4	-4.9	-6.2	-5.5	5.5	5.6
	d3	16.7	89.3	18.3	18.9	3.9	3.8	-4.0	-2.7	-4.0	-3.6	5.5	5.7
^{23}Na	d5	18.7	18.7	21.0	21.8	5.1	5.3	.1	.4	3.6	4.9	5.9	6.2
	s1	15.5	15.4	19.0	19.1	5.2	5.2	-5.7	-4.8	-4.9	-4.0	5.9	6.1
	d3	13.6	13.6	16.6	17.0	5.2	5.2	-4.3	-3.5	-4.2	-3.4	5.7	6.1
^{24}Mg	d5	20.8	21.0	22.3	23.3	5.1	5.3	-1.0	-.4	1.2	2.8	5.8	6.1
	s1	17.6	17.7	20.1	20.2	5.2	5.2	-6.9	-5.9	-6.4	-5.4	5.9	6.0
	d3	15.9	16.1	17.6	18.2	5.2	5.2	-5.9	-4.9	-5.8	-4.9	5.7	6.1
^{25}Mg	d5	19.7	19.8	21.2	22.1	5.4	5.7	4.1	4.2	7.8	10.0	5.9	6.2
	s1	15.8	15.7	18.4	18.5	5.6	5.6	-6.4	-5.2	-5.5	-4.3	5.9	6.1
	d3	13.7	13.9	15.4	16.0	5.6	5.6	-5.9	-4.8	-5.8	-4.6	5.6	6.1
^{26}Mg	d5	19.5	19.4	21.3	22.1	5.7	6.0	21.2	16.9	30.5	29.9	5.8	6.2
	s1	14.9	14.8	17.8	18.0	5.8	5.8	-5.5	-4.0	-3.9	-2.1	5.9	6.1
	d3	12.6	12.8	14.4	15.0	5.8	5.8	-6.1	-4.7	-5.9	-4.5	5.5	6.0
^{25}Al	d5	21.8	22.1	22.3	23.4	5.0	5.2	-4.0	-3.2	-3.3	-1.5	5.7	5.9
	s1	18.7	18.5	19.8	19.9	5.1	5.1	-8.3	-7.3	-8.0	-7.1	5.7	5.8
	d3	16.9	17.1	17.2	17.9	5.1	5.0	-7.3	-6.2	-7.2	-6.2	5.5	5.9
^{26}Al	d5	21.0	21.3	21.5	22.7	5.2	5.5	1.2	1.8	2.5	5.3	5.7	6.0
	s1	17.2	17.1	18.5	18.6	5.4	5.4	-7.7	-6.6	-7.3	-6.1	5.7	5.8
	d3	15.1	15.2	15.5	16.1	5.4	5.4	-7.3	-6.0	-7.3	-6.0	5.4	5.9
^{27}Al	d5	20.6	20.8	21.3	22.5	5.4	5.8	13.6	13.1	16.6	20.8	5.6	6.0
	s1	16.1	16.1	17.6	17.9	5.6	5.6	-6.9	-5.5	-6.1	-4.5	5.6	5.8
	d3	13.8	14.0	14.2	14.9	5.6	5.6	-7.4	-5.9	-7.3	-5.9	5.3	5.8
^{28}Al	d5	20.1	20.1	20.8	22.0	5.5	5.9	38.6	32.5	46.1	50.1	5.4	5.8
	s1	14.9	15.0	16.7	17.0	5.7	5.8	-5.3	-3.3	-3.4	-1.2	5.4	5.7
	d3	12.5	12.7	12.9	13.5	5.7	5.7	-7.4	-5.7	-7.3	-5.6	5.1	5.6

Table 4.2b: Contd....

NUCL	OR	EM1		EM2		SIG-		EP1		EP2		SIG+	
		U	PW	U	PW	U	PW	U	PW	U	PW	U	PW
^{28}Si	d5	22.3	22.7	22.1	23.5	5.1	5.4	15.5	16.5	14.7	20.9	5.3	5.7
	s1	17.6	17.7	18.2	18.5	5.3	5.3	-8.4	-7.2	-8.2	-6.8	5.3	5.5
	d3	15.3	15.7	14.7	15.5	5.3	5.2	-8.9	-7.4	-9.0	-7.5	5.0	5.4
^{29}Si	d5	21.2	21.5	21.0	22.5	5.2	5.6	27.5	29.1	25.8	38.1	5.1	5.6
	s1	16.1	16.1	16.7	17.0	5.4	5.4	-7.2	-5.5	-6.6	-4.7	5.1	5.3
	d3	7.8	13.8	13.0	13.5	5.3	5.3	-9.7	-6.9	-8.8	-6.9	4.8	5.3
^{30}Si	d5	20.4	20.7	20.3	21.8	5.1	5.7	57.2	59.3	54.0	82.1	4.8	5.4
	s1	15.2	15.1	15.9	16.1	5.4	5.5	-4.7	-1.5	-3.1	.9	4.8	5.4
	d3	12.7	12.5	12.0	12.1	5.3	5.3	-8.6	-6.4	-8.8	-6.6	4.6	5.3
^{29}P	d5	23.3	23.8	22.2	23.7	4.7	5.0	10.2	13.8	5.1	13.3	4.9	5.2
	s1	18.6	18.4	18.1	18.3	4.8	4.9	-10.3	-9.4	-10.6	-9.4	4.8	5.0
	d3	16.3	16.2	14.7	15.1	4.8	4.9	-10.2	-8.5	-10.3	-8.7	4.5	4.9
^{30}P	d5	22.5	23.0	21.5	23.1	4.7	5.2	28.2	33.6	18.5	34.5	4.7	5.1
	s1	17.4	17.3	17.0	17.2	4.9	5.0	-9.1	-7.8	-9.5	-7.8	4.7	4.9
	d3	14.9	14.7	13.3	13.5	4.9	4.8	-10.1	-8.1	-10.4	-8.4	4.4	4.7
^{31}P	d5	21.9	22.4	20.9	22.7	4.7	5.2	72.0	87.1	51.0	95.3	4.4	4.9
	s1	16.6	16.5	16.4	16.7	5.0	5.1	-6.5	-3.7	-7.0	-3.4	4.4	4.7
	d3	14.0	13.7	12.3	12.3	4.9	4.9	-10.0	-7.8	-10.4	-8.1	4.2	4.5
^{32}S	d5	23.1	22.9	21.2	23.0	4.1	4.7	86.5	100.0	36.7	88.9	3.8	4.3
	s1	17.8	17.6	16.5	16.8	4.4	4.5	-8.9	-7.3	-11.8	-9.1	3.8	4.2
	d3	15.1	14.2	12.3	11.9	4.2	4.2	-11.3	-8.8	-12.0	-9.4	3.6	3.8
^{33}S	d5	21.8	22.3	20.0	21.9	4.3	4.7	87.3	100.0	13.1	100.0	3.4	4.0
	s1	17.0	16.7	15.7	16.1	4.2	4.4	-7.6	-3.4	-12.9	-7.0	3.5	3.9
	d3	14.2	12.7	11.5	10.5	4.0	4.0	-10.9	-7.9	-12.6	-9.1	3.2	3.5
^{34}S	d5	20.8	21.2	19.0	21.0	3.9	4.7	100.0	100.0	-38.4	100.0	3.0	3.2
	s1	16.4	15.9	15.1	15.5	4.1	4.3	-6.1	2.5	-16.6	-5.6	3.2	3.4
	d3	13.6	11.3	10.9	9.2	3.8	3.7	-10.5	-7.0	-14.1	-9.5	2.8	3.0
^{33}Cl	d5	24.1	24.9	21.5	23.5	3.4	4.0	100.0	100.0	14.6	91.1	3.1	3.6
	s1	18.8	18.4	16.7	17.0	3.7	3.9	-11.1	-10.2	-15.7	-13.7	3.1	3.5
	d3	16.1	14.7	12.3	11.4	3.4	3.4	-12.6	-9.8	-13.6	-10.5	2.8	3.1
^{35}Cl	d5	22.1	22.8	19.5	21.8	3.2	3.9	100.0	100.0	100.0	100.0	2.3	2.7
	s1	17.6	17.1	15.5	15.8	3.5	3.6	-7.3	2.6	-30.6	-36.4	2.4	2.6
	d3	14.8	12.2	11.0	8.9	2.9	2.7	-11.8	-7.8	-16.4	-11.4	2.1	2.0
^{36}Ar	d5	23.6	24.6	20.2	22.9	2.4	3.2	100.0	100.0	100.0	3.2	1.6	6.0
	s1	18.6	18.0	15.9	15.8	2.1	2.8	-3.3	46.1	-70.7	2.8	1.8	2.0
	d3	16.2	13.2	11.0	8.0	2.0	1.8	-12.9	-8.3	-18.6	-1.3	1.3	2.0

Table 4.3: Occupancy dependent single particle energies (-Ej) and ground state energies (s-d shell).

NUCL		-Ej (PROTONS)			-Ej (NEUTRONS)			G.STATE
		d5/2	s1/2	d3/2	d5/2	s1/2	d3/2	ENERGIES
20	U	8.5	6.2	2.4	8.5	6.2	2.4	-39.4
Ne	PW	8.4	5.6	2.3	8.4	5.6	2.3	-39.4
22	U	12.1	8.9	5.9	9.3	5.9	2.9	-61.7
Ne	PW	11.8	7.8	5.3	9.0	5.5	2.4	-62.1
23	U	12.4	8.8	5.9	11.0	7.4	4.5	-75.4
Na	PW	12.2	7.8	5.3	10.7	6.6	3.8	-76.1
24	U	12.7	8.7	6.1	12.7	8.7	6.1	-91.4
Mg	PW	12.5	7.8	5.3	12.5	7.8	5.3	-92.4
26	U	15.8	11.6	9.1	13.2	8.8	6.4	-114.8
Mg	PW	15.9	10.5	8.1	13.0	7.9	5.3	-116.7
27	U	16.0	11.5	9.2	14.7	10.2	7.9	-127.7
Al	PW	16.2	10.4	8.0	14.8	9.1	6.7	-130.3
28	U	16.3	11.5	9.4	16.3	11.5	9.4	-144.3
Si	PW	16.5	10.4	8.2	16.5	10.4	8.2	-147.6
30	U	19.0	14.6	12.0	16.4	11.9	9.5	-163.6
Si	PW	19.5	13.7	10.2	16.8	10.8	7.9	-167.7
31	U	19.1	14.8	12.0	17.8	13.4	10.8	-179.4
P	PW	19.6	14.1	10.1	18.3	12.6	9.0	-184.6
32	U	19.1	15.0	12.1	19.1	15.0	12.1	-190.1
S	PW	19.6	14.6	9.9	19.6	14.6	9.9	-195.1
34	U	21.8	17.7	14.5	19.2	15.3	12.3	-206.5
S	PW	22.6	17.3	11.5	19.8	14.9	9.3	-210.3
35	U	21.8	17.9	14.6	20.5	16.7	13.4	-218.1
Cl	PW	22.6	17.6	11.1	21.2	16.5	10.1	-222.3
36	U	21.8	18.1	14.6	21.8	18.1	14.6	-230.3
Ar	PW	22.9	17.5	10.8	22.9	17.5	10.8	-232.8

Table 4.4: Coulomb corrected (-Ej) for proton orbits (s-d shell)

Nucl	d5/2			s1/2			d3/2		
	U	PW	Expt	U	PW	Expt	U	PW	Expt.
^{24}Mg	7.4	7.3	7.8	3.4	2.5	2.9	0.8	0.1	1.8
^{26}Mg	10.6	10.7	10.1	6.4	5.3	7.6	3.9	2.9	5.9
^{27}Al	10.5	10.7	11.5	6.0	4.9	5.1	3.7	2.5	4.5
^{28}Si	10.4	10.6	9.6	5.6	4.5	6.2	3.5	2.3	3.4
^{30}Si	13.2	13.7	12.1	8.8	7.9	8.9	6.2	4.4	6.5
^{31}P	13.0	13.5	13.3	8.7	8.0	7.5	5.9	4.0	4.2
^{32}S	12.6	13.1	12.6	8.5	8.1	8.2	5.6	3.4	3.7
^{34}S	15.4	16.2	12.5	11.3	10.9	10.0	8.1	5.1	6.6
^{35}Cl	15.1	15.9	12.4	11.2	10.9	9.2	7.9	4.4	5.6
^{36}Ar	14.8	15.9	12.8	11.1	10.5	8.9	7.6	3.8	5.9

Expt: Experimental results from reference no. 37.

Figure captions:

Figures 4.1 a-d: Ground state proton and neutron occupancies for various nuclei, using the PW interaction and the universal s-d interaction alongwith the experimental results. R5 and R8 refer to the experimental results as given in reference nos. 17 and 37 respectively. Occupancies for isotopes are connected using lines/dashes for different interactions, which are identified through different symbols.

Figures 4.1 e-g: Proton effective single particle energies for different nuclei using the PW and the universal s-d interctions alongwith the experimental results from reference no 37.

Figures 4.2 a-b: Locations of SNT centroids and ground-state energies of the target and the final nuclei. The ground state energies have been calulated using the Ratcliff's procedure /17/. Target nucleus in (a) is ^{24}Mg and in (b) is ^{27}Al; (i) particle removal using bivariate gaussian strength function, (ii) particle removal using polynomial expansion (iii) particle addition using bivariate gaussian strength function, (iv) particle addition using polynomial expansion. Left half of each figure corresponds to the universal s-d interaction and the right half is for the PW interaction. Proton transfer results are given by full-line (——) and the neutron transfer results are given by dashed line(------). Coulomb correction has not been incorporated. Centroids are labelled by orbit angular momentum and 2*j value of the orbit.

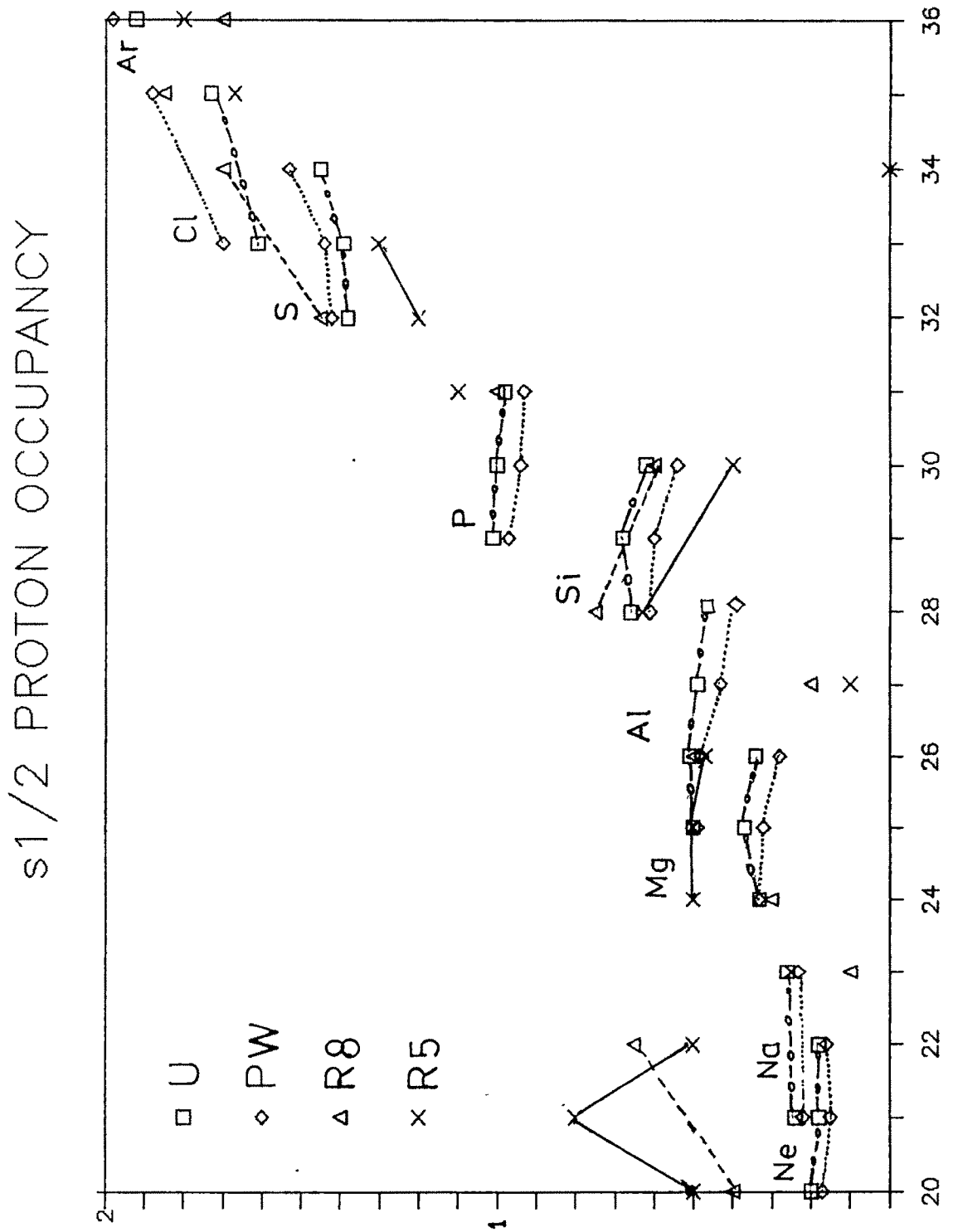
s1/2 PROTON OCCUPANCY
U
PW
R8
R5
Ar
Cl
S
P
Si
Al
Mg
Na
Ne
2
1
20
22
24
26
28
30
32
34
36
MASS NUMBER

Fig 4.1a

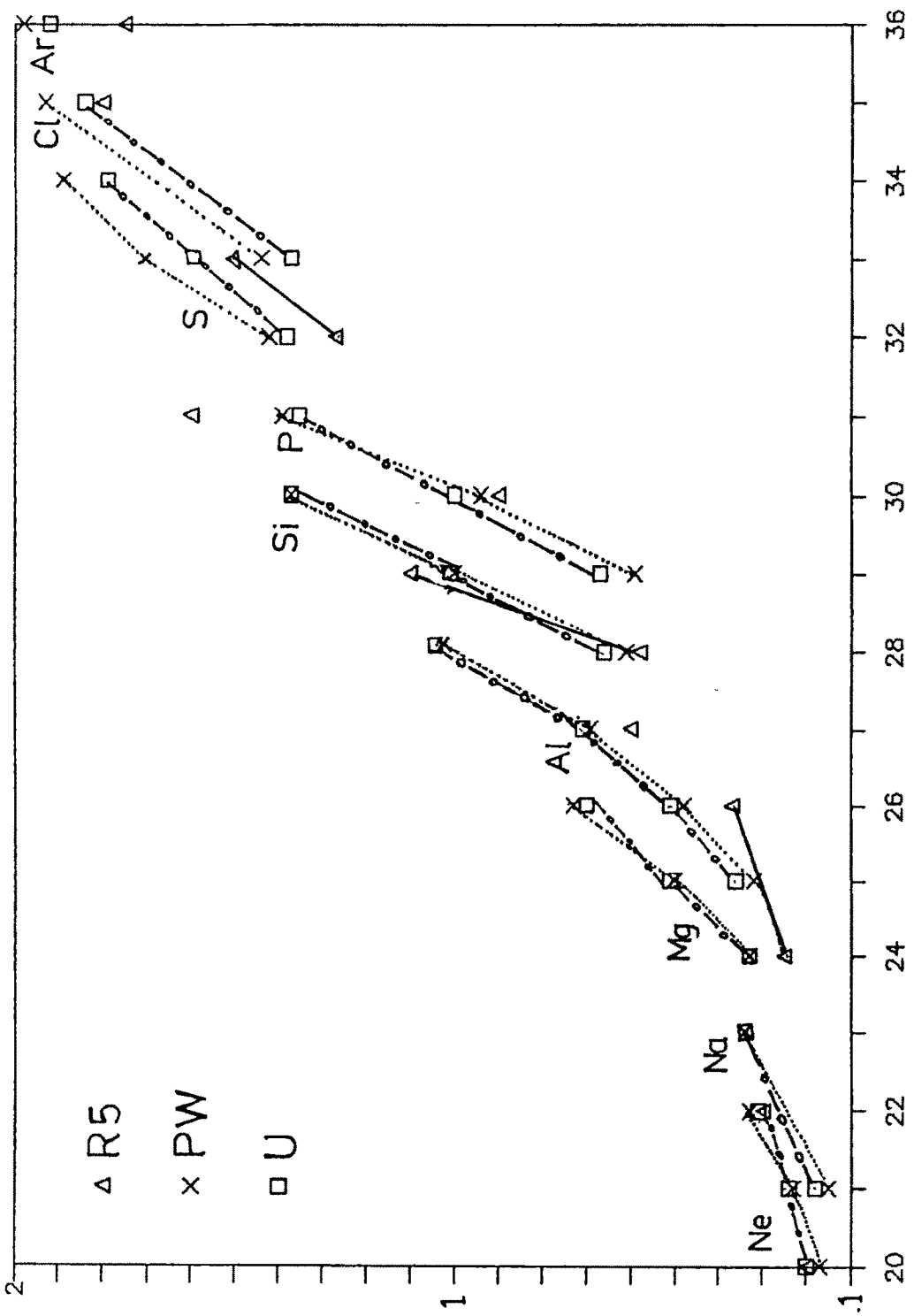
s1/2 NEUTRON OCCUPANCY
Ar
Cl
S
P
Si
Al
Mg
Na
Ne
R5
PW
U
2
1
.1
20
22
24
26
28
30
32
34
36
MASS NUMBER

Fig. 4.1b

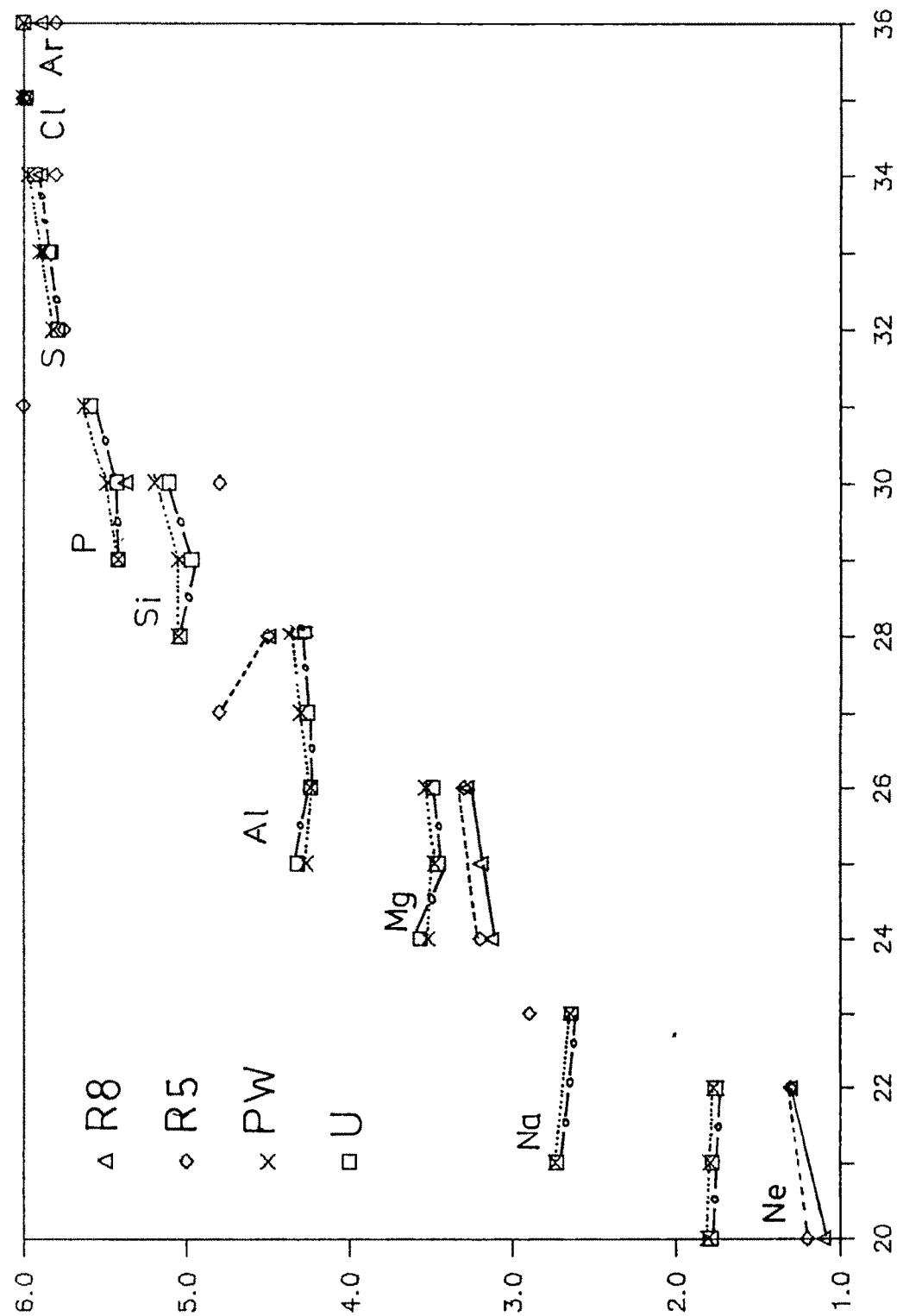
d5/2 PROTON OCCUPANCY
6.0
5.0
4.0
3.0
2.0
1.0
20
22
24
26
28
30
32
34
36
MASS NUMBER
R8
R5
PW
U
Ne
Na
Mg
Al
Si
P
S
Cl
Ar

Fig. 4.1c

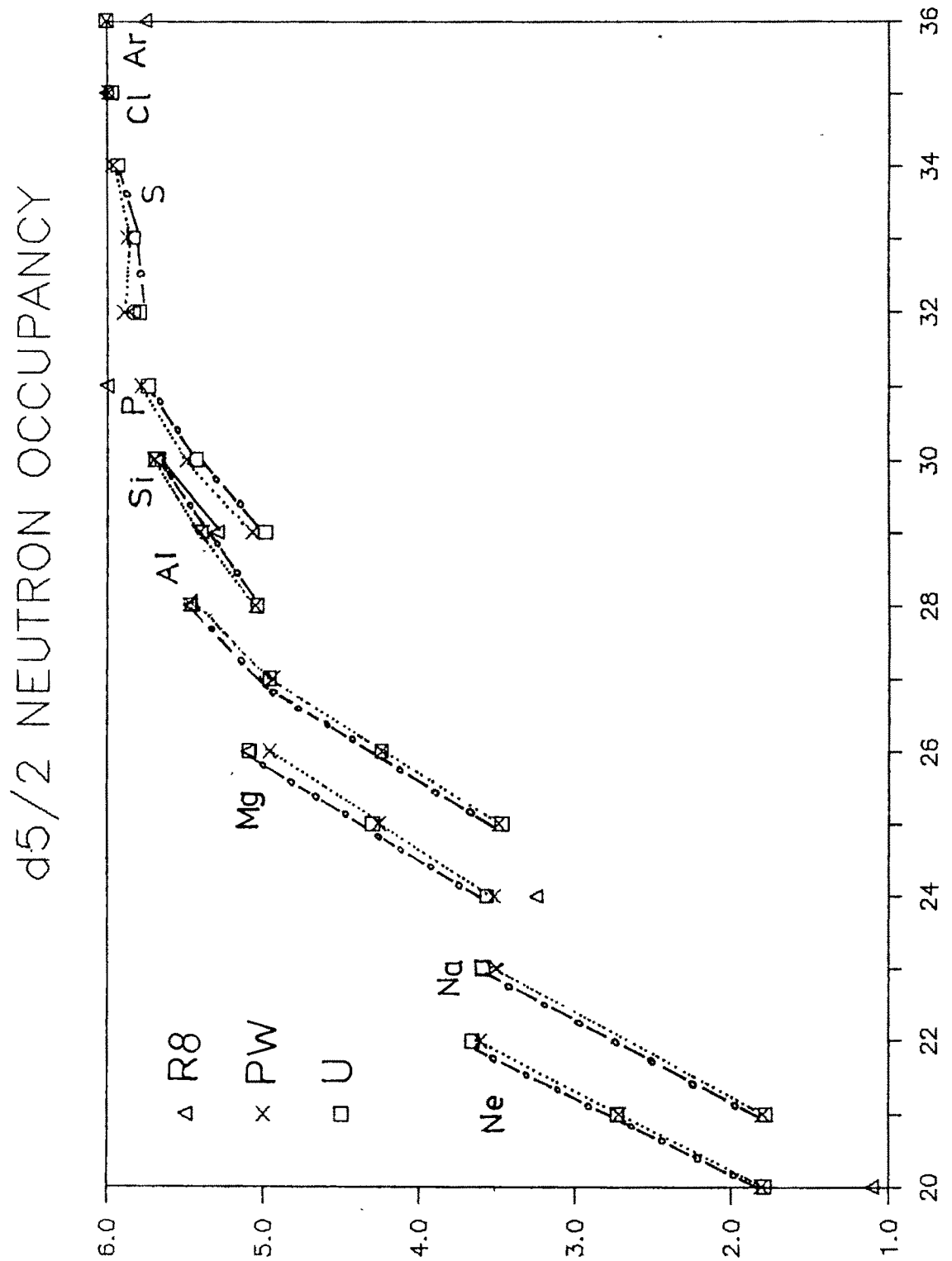
d5/2 NEUTRON OCCUPANCY
6.0
5.0
4.0
3.0
2.0
1.0
20
22
24
26
28
30
32
34
36
MASS NUMBER
Ne
Na
Mg
Al
Si
P
S
Cl
Ar
R8
PW
U

Fig. 4.1d

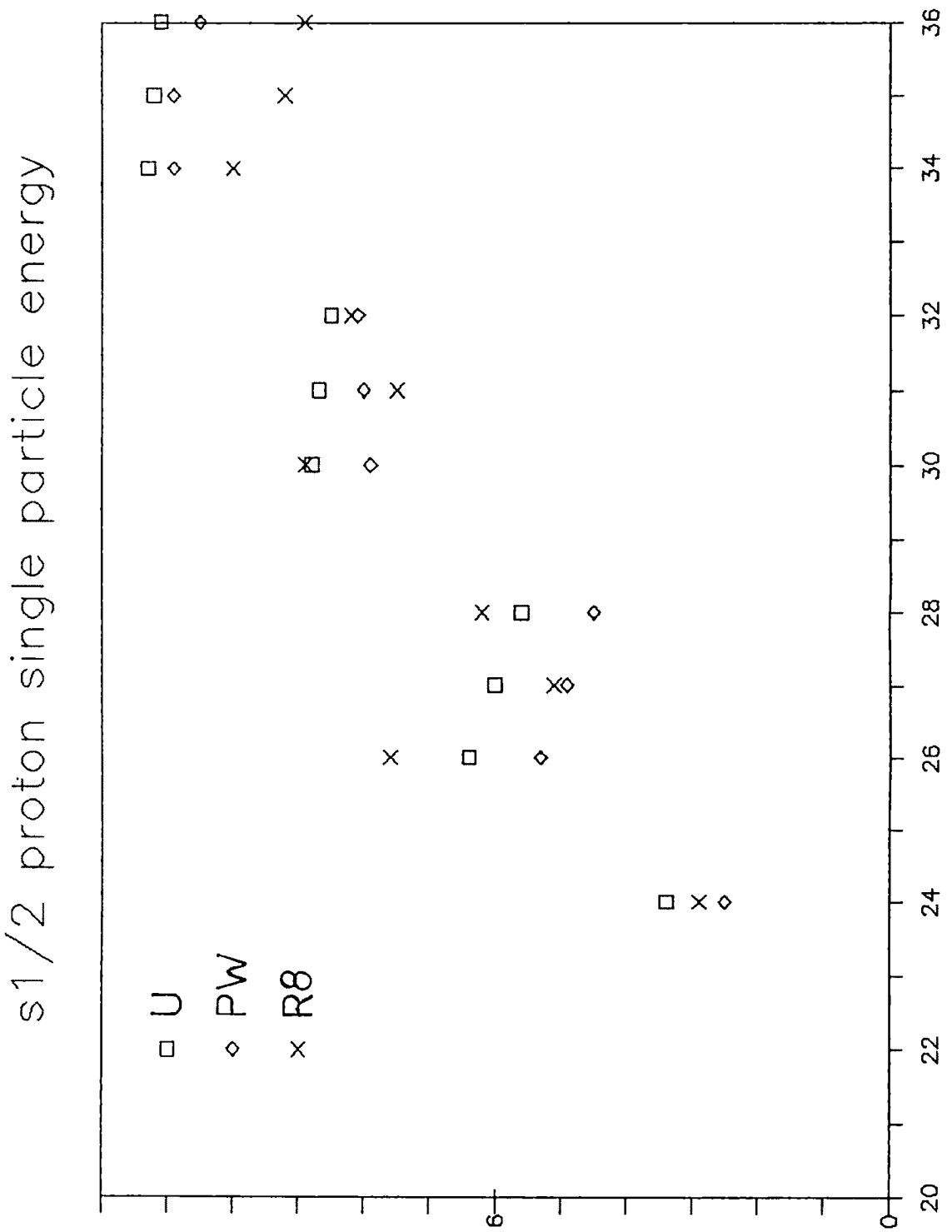
s1/2 proton single particle energy
U
PW
R8
0
6
20
22
24
26
28
30
32
34
36
MASS NUMBER

Fig. 4.1e

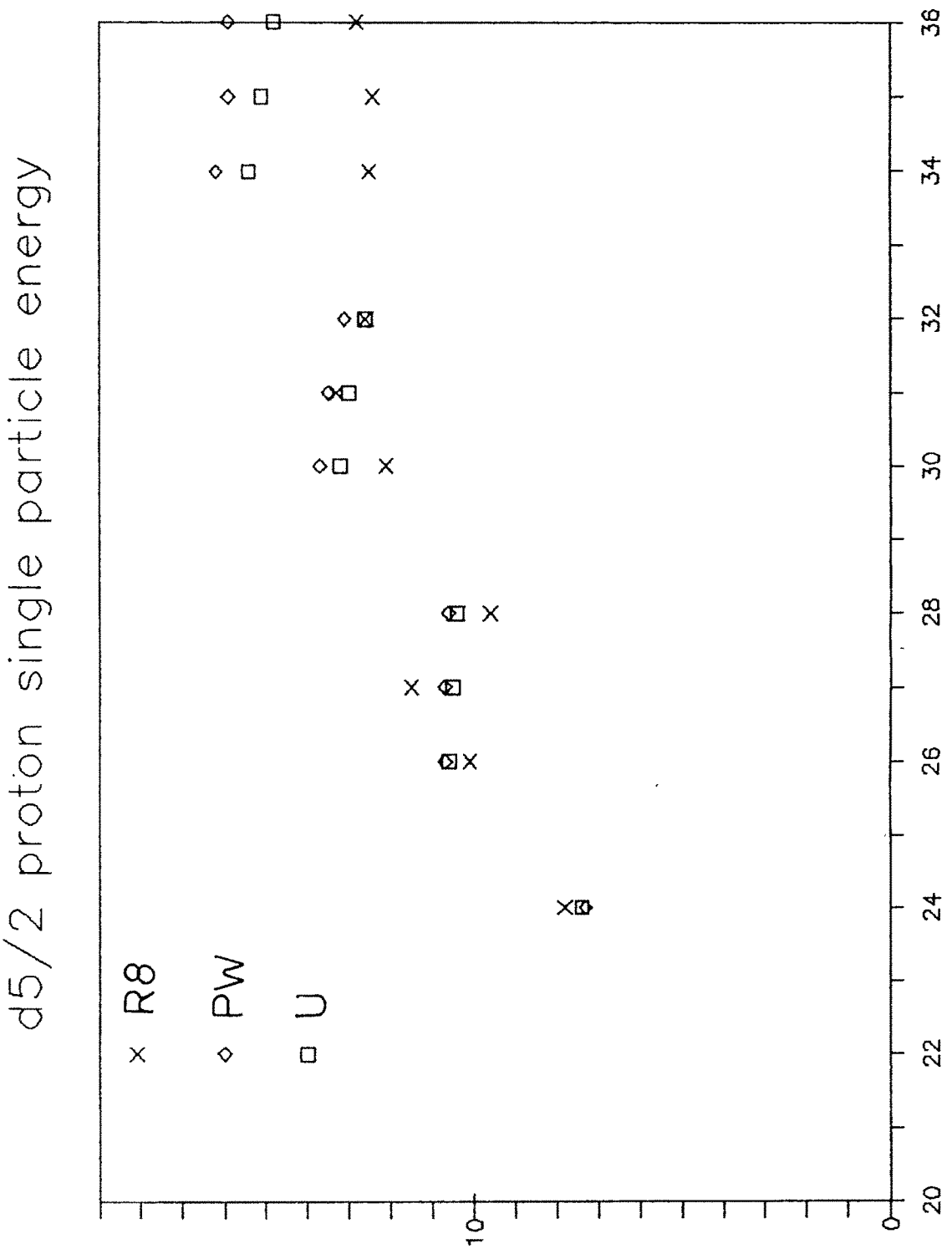
d5/2 proton single particle energy
R8
PW
U
10
0
20
22
24
26
28
30
32
34
36
MASS NUMBER

Fig. 4.1f

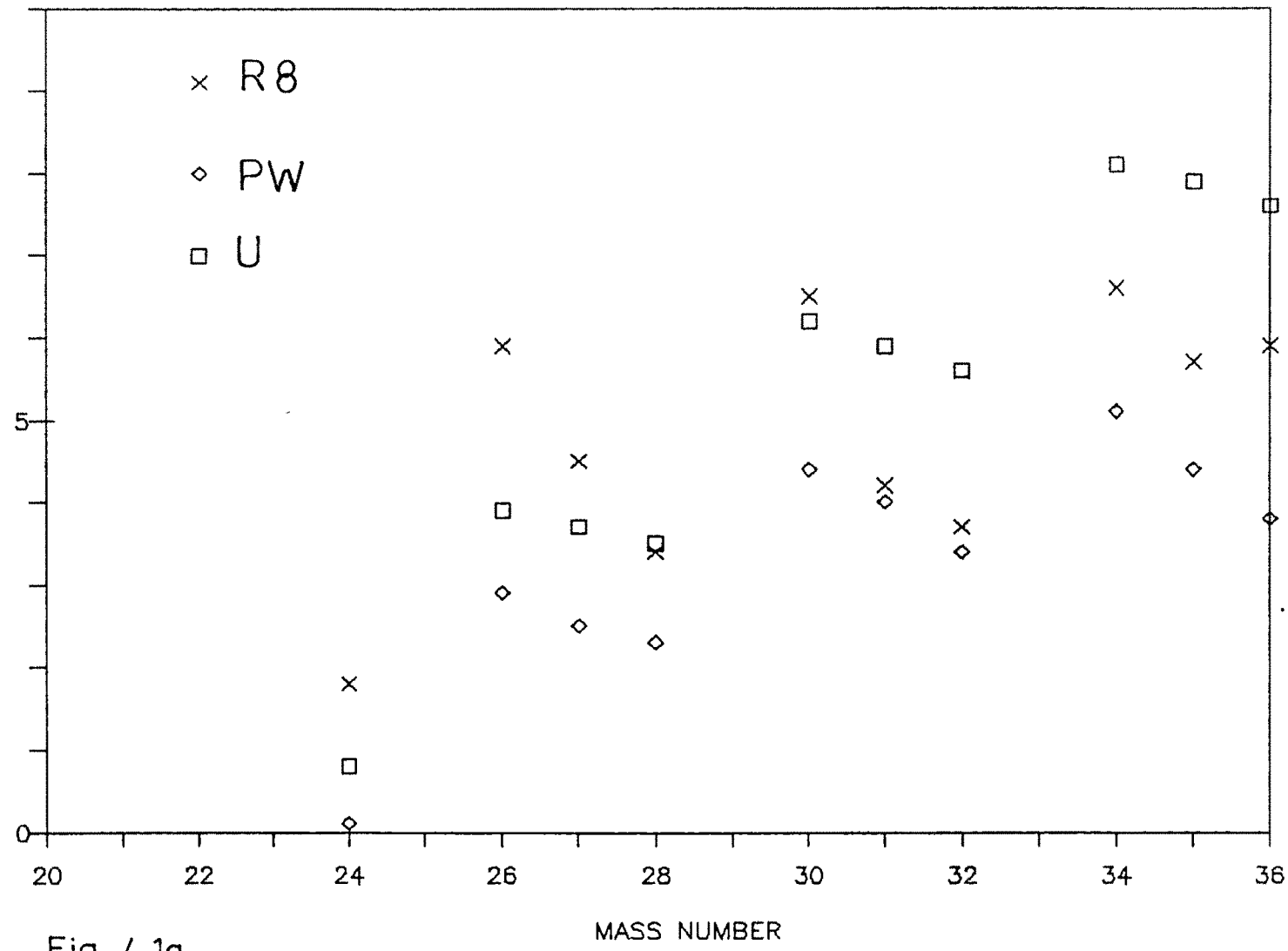
d3/2 proton single particle energy
R8
PW
U
5
0
20
22
24
26
28
30
32
34
36
MASS NUMBER

Fig. 4.1g

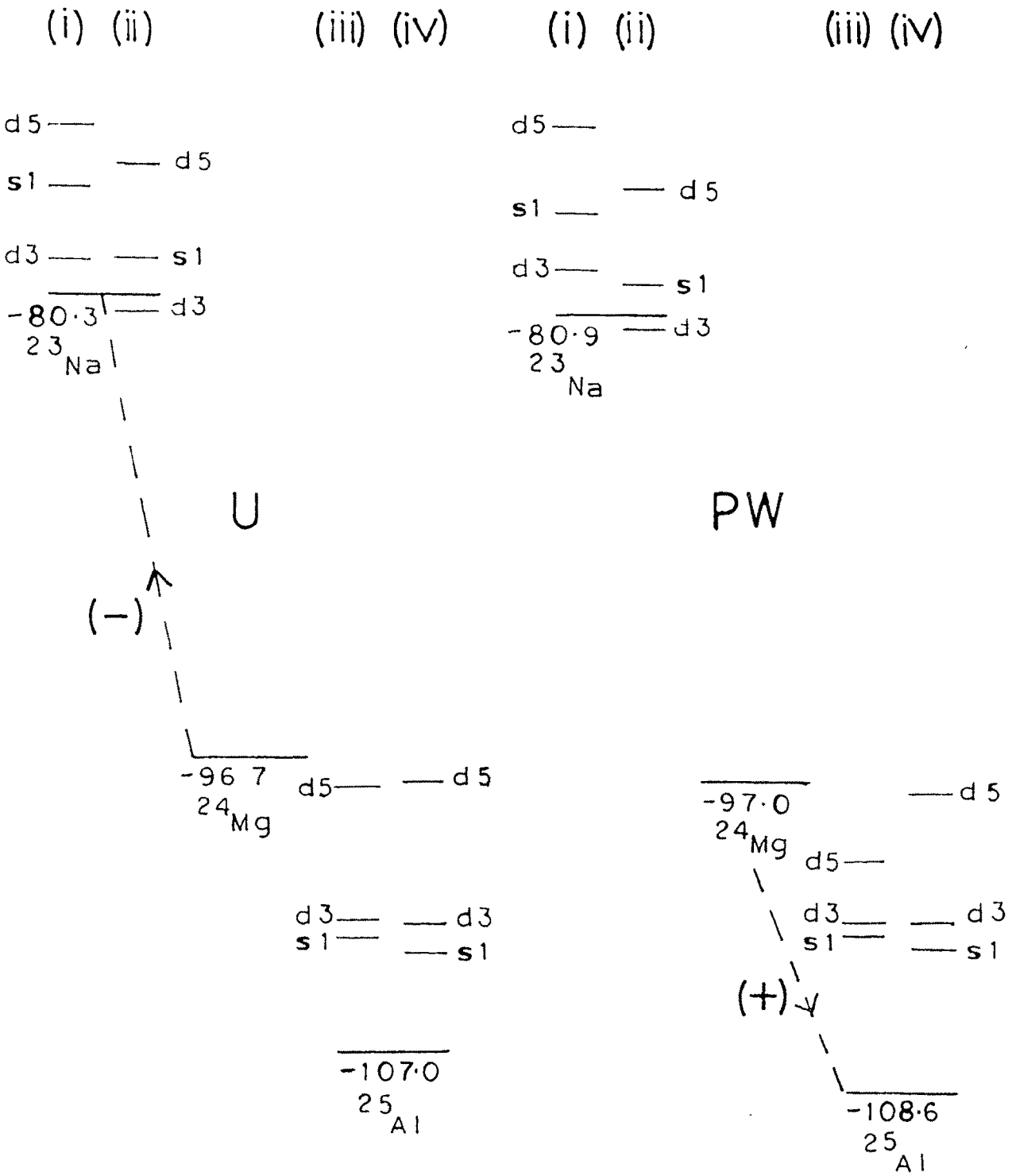
(i) (ii) (iii) (iv)
d5
s1
d3
d5
s1
d3
-80·3
23 Na
U
(-)
-96 7
24 Mg
d5
d5
d3
s1
d3
s1
-107·0
25 Al
(i) (ii) (iii) (iv)
d5
s1
d3
d5
s1
d3
-80·9
23 Na
PW
-97·0
24 Mg
d5
d5
d3
s1
d3
s1
(+)
-108·6
25 Al

Fig.42a

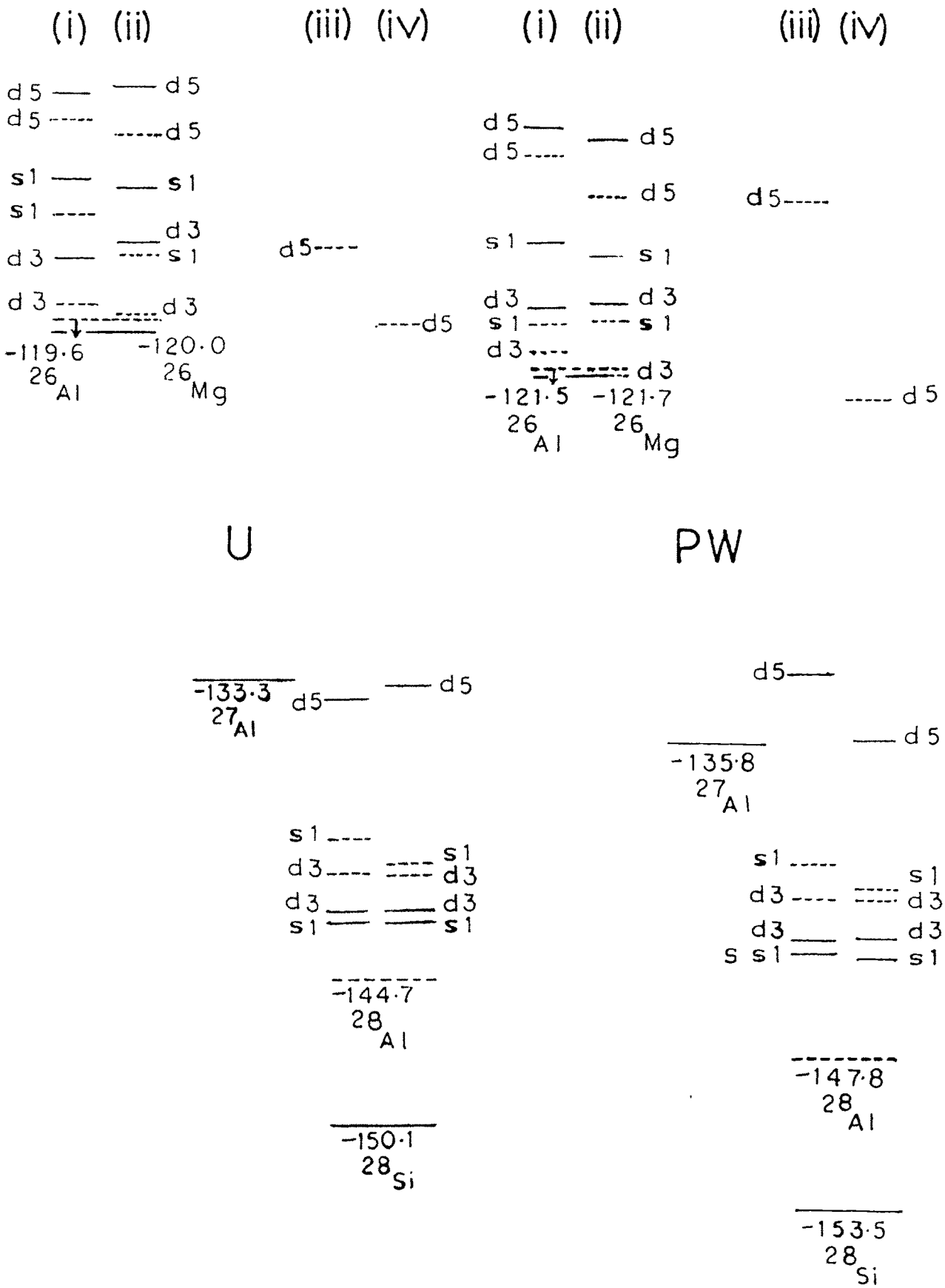
(i) (ii) (iii) (iv)
d5
d5
s1
s1
d3
d3
d3
d5
-119·6
26Al
-120·0
26Mg
(i) (ii) (iii) (iv)
d5
d5
d5
s1
s1
d3
s1
d3
d3
d5
d5
-121·5
26Al
-121·7
26Mg
U
PW
-133·3
27Al
d5
d5
d5
-135·8
27Al
s1
d3
s1
d3
d3
s1
s1
d3
d3
s1
-144·7
28Al
-147·8
28Al
-150·1
28Si
-153·5
28Si

Fig. 4.2 b.

Discussion

Experimental values of ground-state proton occupancies have been reported recently by Ishkhanov et. al. /37/. Similar compilation of experimental data has also been reported earlier /17/ for proton-neutron occupancies. It should be kept in mind that experimental spectroscopic factors are uncertain by about 20% to 30% in their relative values because of ambiguities in the optical model parameters, finite range adjustments, nonlocality corrections etc. In addition, there is another source of ambiguity for sum-rule evaluation: the missing strength at high excitation energy. Secondly, it is not always possible to separate $\ell=2$ transfer strength into its $d_{5/2}$ and $d_{3/2}$ components. Fig.4.1 is a graphical representation of the data in Table-4.1 Both the effective interactions used give almost similar results. For proton occupancies, the two sets of experimental compilations are at variance in several cases; this however is normal, providing justification for the comments on experimental uncertainty. Fig.4.1a displays the variation of $s_{1/2}$-proton occupancy using the two effective interactions and the experimental values. Except for a few nuclei in the lower s-d shell, the calculated results seem to agree (within assumed experimental error of 25%) with the experimental values; the universal s-d interaction being slightly better than the PW interaction. Fig.4.1b is a similar plot for $s_{1/2}$ neutron occupancies, experimental values in this case have been taken from /17/. It seems that the calculated neutron occupancies agree much better with the experimental values again within the limits of error values mentioned. Here also, the universal s-d interaction is a shade better than the PW interaction. A comparison of calculated $\ell=2$ occupancy with experimental results is redundant, once the $s_{1/2}$ occupancy results have been analysed. However, we can still

talk about decomposition of the strength into $d_{5/2}$ and $d_{3/2}$ components, but not with the same confidence as in the case of $s_{1/2}$ orbit, due to ambiguity in experimental identification of the strength bifurcation into these orbits. High occupancy values of $d_{5/2}$ orbit seem to agree well with the calculated results (within acceptable error limits) except in the case of light nuclei (^{20}Ne and ^{22}Ne) where the calculated values are considerably higher than the experimental results. The low occupancy of $d_{3/2}$ orbit would provide a tough test. The universal s-d interaction gives rise to slightly higher $d_{3/2}$ occupancy in upper s-d shell compared to the values given by the PW interaction. The trend is reversed in the lower s-d shell. This is the result of larger $d_{5/2}$-$d_{3/2}$ difference (spin-orbit splitting) in the external single particle energies for the universal s-d interaction (5.60 MeV) as compared to the 5.08 MeV in the case of PW interaction. Induced single particle energies /3/ however reverse the situation in upper s-d shell; for example the spin orbit splitting in μ = 1 part of the interaction at ^{36}Ar for universal s-d interaction is 7.2 MeV while the same number for PW interaction is 13.3 MeV. This indicates large contribution of spin-orbit splitting in the PW interaction compared to the universal s-d interaction. For ^{22}Ne, ^{28}Mg, ^{32}S, ^{34}S, ^{35}Cl and ^{35}Ar, calculated values of the $d_{3/2}$ orbit occupancies match well with the experimental results.

Table-4.1 gives the ground state pickup and stripping centroids and widths. Here, due to the absence of any experimental data, we restrict to some general comments and hope that this would stimulate a thorough experimental analysis in this region. Also, there are no exact shell-model calculations available for testing the accuracy of the two methods employed. Figure 4.1, which is a pictorial representation of the data in Table-4.1, gives the locations

of the particle removal and the addition centroids and the respective ground-state energies of the target and the final nuclei. Both the interactions employed give similar results (which deviate from one another by small amounts) pointing to the gross similarity of the two interactions. Also the two methods of evaluating the centroids of strength distributions (though not giving identical results) do not differ from one another appreciably; thereby giving us licence to use the heuristic formula for the strength function which can be described now as a superposition of bivariate gaussians with constant correlation coefficient as proposed in /34/ by Prof. French. This approach will be of immense use in huge spaces extending over many harmonic oscillator orbits. It is true that sometimes the calculated values of strength centroids lie below the respective final nucleus ground states. This is because of the inherent limitation of the finite polynomial expansion resulting due to truncation of the expectation value expression. On the other hand, one can invert the argument and say that in such cases, most of the strength would be concentrated within few states near the final nucleus ground state. Secondly, the widths of the strength distributions are small compared to the spread of the configuration intensity over the energy axis (average configuration width in ^{24}Mg = 8.2 MeV). This also indicates that the single particle state is not spread over large energy domain, giving credence to the single-particle picture. The location and width together indicate the range of energy in which most of the particle transfer strength is concentrated, and hence gives an indication of the excitation energy to which an experiment must be conducted in order to exhaust most of the strength. As discussed earlier (equation 32), the particle addition centroids and the particle removal centroids with reference to a particular target state are related to one another through occupancies of the target state and average two-body matrix

elements. The right hand side of the equation 32 is the occupancy dependent single-particle energy (E_j) of the target nucleus. These E_j's indirectly depend upon the excitation energy also, since the occupancies vary with energy. Their values in the ground-state region of the respective nuclei for proton and neutron orbits using both the interactions are presented in Table-4.3. An analysis /38/ of this type in 2s-1d and $f_{7/2}$ shell using PW interaction and cross shell matrix elements from Kuo-Brown interaction was attempted without taking into account the ground state occupancies properly. The energy span between $d_{5/2}$ and $d_{3/2}$ orbits seems to be slowly increasing as the shell is gradually being filled up. $E_{d5/2}$ falls much faster than $E_{d3/2}$. There is however no crossing of energy levels. Thus the $d_{5/2}$ (proton or neutron) gets progressively bound more and more as the shell is being filled. $E_{d5/2}$ orbit energy falls from -8.5 MeV in ^{20}Ne to -21.8 MeV in ^{36}Ar for universal s-d interaction. For $s_{1/2}$ orbit, the change is from -8.2 MeV to -18.1 MeV, while for $d_{3/2}$ orbit it varies from -2.4 MeV to -14.8 MeV. So the energy span between $d_{5/2}$ to $d_{3/2}$ orbits for the universal s-d interaction has increased from 6.1 MeV to 7.2 MeV. For the PW interaction, the corresponding increase in energy span between $d_{5/2}$ and $d_{3/2}$ orbits is more i.e. from 6.1 MeV in ^{24}Ne to 12.1 MeV in ^{36}Ar. Again the splitting increases much more rapidly for the PW interaction as compared to the universal s-d interaction. The proton and neutron energies are symmetric as the effective interactions are isospin conserving. The coulomb interaction however breaks this symmetry and hence the calculated values have to be corrected in order to be compared with the experimental results. Ishkhanov et. al. have evaluated values of these for proton orbits using experimental data. The calculated values given in Table-4.4 have been corrected for coulomb energy using the standard formula for coulomb energy. The calculated values agree

quite well with the experimental values, with minor deviations in few cases. This is remarkable considering the fact that the errors in experimental evaluation are compounded. The universal s-d interaction at this stage seems to be much superior than the PW interaction. This can be easily seen by comparing $d_{5/2}$ and $d_{3/2}$ splittings produced by the two interactions with the experimental values. The PW interaction gives too large values for the separation between $E_{d5/2}$ and $E_{d3/2}$. Experimentally, the addition of a neutron pair to isotopes of magnesium, silicon and sulphur weakens the splitting of 1d level/37/. Both the interactions fail to reproduce the trend. This can be traced to the nature of the j = 1 part of the interaction (the induced single-particle energies /3/) and is clearly an interaction dependent result. For both the interactions splitting between induced single particle energies between $d_{5/2}$ and $d_{3/2}$ orbits (for protons as well as for neutrons) can be seen to be increasing with proton and neutron numbers. In the universal s-d interaction, this increase is damped due to the factor of $(18/A)^3$ in the two body matrix elements. However, one can conclusively see that the universal s-d interaction compares much better with the experimental data than the PW interaction. Thus the method provides a nice way of selecting a proper effective interaction.

(b) f-p shell

A thorough study on ground state binding energies and ground state occupancies in proton-neutron scalar and configuration spaces has been carried out for various nuclei in the f-p shell by Kota and Potbhare /18/ using five different effective interactions. Here, we carry out an extension to their work, using four of those five effective interactions.

The dimensionalities of spaces involved in the calculations being extremely large, it has not been possible to calculate the centroids and widths of particle removal and particle addition strengths for most of the nuclei in the f-p shell. However, the occupancy-weighted difference between centroids of the particle removal strength and the particle addition strength, which corresponds to the effective single particle energy, can be easily evaluated. These have been calculated for different nuclei using the occupancy values of /18/. The effective interaction used are either renormalized or empirically modified versions of the bare Kuo-Brown interaction .

1 The KB3p-1h effective interaction is obtained from the bare Kuo-Brown interaction by renormalising it for three particle - one hole excitation above the ^{40}Ca core/39/.

2 The MWH effective interaction is obtained by changing few matrix elements of the KB3p-1h effective interaction so as to fit calcium isotopes data /40/. Changes made in KB3p-1h are the following:

(i) Matrix elements of $\langle f_{7/2}^2 \; J|V|f_{7/2}^2 \; J\rangle$ for J = 0, 2 were made more attractive by 0.3 MeV and

(ii) Matrix elements of $\langle f_{7/2}p_{3/2} \; J|V|f_{7/2}p_{3/2} \; J\rangle$ were made repulsive by 0.3 MeV so as to raise their centre of gravity from (-0.1) to 0.2 MeV.

3 The MWH2 effective interaction is obtained from further modification of the MWH interaction. Here, 250 KeV is added to all diagonal matrix elements of the type $\langle f_{7/2}p_{1/2} \; J|V|f_{7/2}p_{1/2} \; J\rangle$ & $\langle f_{7/2}f_{5/2} \; J|V|f_{7/2}f_{5/2} \; J\rangle$ to raise the centre of gravity of interaction of $p_{1/2}$ and $f_{5/2}$ orbits with $f_{7/2}$ orbit.

4 The KB10 interaction is originally a 10-orbit interacion spanning orbits from $1s_{1/2}$ to $1f_{5/2}$. The four-orbit f-p shell matrix elements are extracted from them.

The single particle energies for all four effective interactions are taken from the spectrum of ^{41}Ca, the values being -8.364, -6.264, -4.464 and -1.864 MeV for $f_{7/2}$, $p_{3/2}$, $p_{1/2}$ and $f_{5/2}$ orbits respectively. Table 4.5 gives values of theoretically obtained effective single particle energies for protons and neutrons. There are eight columns corresponding to four proton and four neutron orbits. Results for the four effective interactions are given one below the other, for different nuclei starting from ^{46}Ti. In order to compare the theoretical values of single particle energy with experimental results, the coloumb correction has to be taken care of in proton energy values, just as in the case of s-d shell. The proton single particle energies corrected for coloumb repulsion are presented in Table 4.6. Experimental single particles energies of Boboshin et.al. /41/ are given in Table 4.7, and plotted alongwith the theoretical results in Fig 4.3a,b. Fig4.3c-d show the neutron single particle energies.

It has been argued /41/ that single particle energies give indications of shell structure within the nucleus, as seen through the magic number dependence of energy difference between $f_{7/2}$-$p_{3/2}$ orbits. This difference is therefore calculated for the four effective interactions and shown together with the experimental energy difference in Table 4.8. There are no experimental results for neutron single particle energies, however, the theoretical energy difference between $f_{7/2}$-$p_{7/2}$ orbits is also given for neutron single particle energies.

Table 4.5: Theoretical proton and neutron effective single particle energies (-Ej) for f-p shell nuclei.

Nucl	Int	Proton orbits				Neutron orbits			
		f5/2	f7/2	p3/2	p1/2	f5/2	f7/2	p3/2	p1/2
	A	-5.99	-11.39	-8.64	-7.21	-4.59	-10.21	-7.76	-6.26
46	B	-6.03	-11.65	-7.36	-7.18	-4.62	-10.52	-6.17	-6.25
Ti	C	-5.03	-11.65	-7.36	-6.18	-3.37	-10.52	-6.17	-5.00
	D	-9.08	-13.10	-10.40	-9.28	-7.32	-11.82	-9.42	-8.16
	A	-7.67	-12.75	-9.91	-8.65	-4.95	-10.44	-8.04	-6.66
48	B	-7.84	-13.10	-8.17	-8.41	-5.04	-10.85	-5.79	-6.53
Ti	C	-6.62	-13.10	-8.15	-7.17	-3.32	-10.85	-5.78	-4.81
	D	-11.71	-15.11	-12.43	-11.59	-8.27	-12.60	-10.35	-9.18
	A	-9.08	-14.02	-11.45	-10.40	-5.16	-10.65	-8.35	-7.15
50	B	-9.47	-14.49	-9.25	-9.76	-5.36	-11.14	-5.62	-6.85
Ti	C	-8.14	-14.48	-9.13	-8.33	-3.27	-11.10	-5.54	-4.73
	D	-14.05	-17.02	-14.76	-14.73	-9.06	-13.36	-11.34	-10.29
	A	-8.02	-12.96	-10.16	-8.98	-6.69	-11.82	-9.17	-7.94
50	B	-8.24	-13.45	-7.80	-8.70	-6.86	-12.33	-6.62	-7.76
Cr	C	-6.55	-13.42	-7.75	-6.98	-4.92	-12.30	-6.57	-5.80
	D	-12.68	-15.95	-13.27	-12.41	-11.00	-14.72	-12.19	-11.15
	A	-9.41	-14.25	-11.70	-10.71	-6.88	-12.05	-9.54	-8.47
52	B	-9.78	-14.86	-8.93	-10.01	-7.11	-12.61	-6.49	-8.02
Cr	C	-8.02	-14.77	-8.85	-8.21	-4.85	-12.48	-6.41	-5.76
	D	-15.09	-17.97	-15.44	-14.79	-11.83	-15.54	-13.13	-12.12
	A	-10.57	-15.46	-13.44	-12.66	-6.91	-12.23	-9.95	-9.08
54	B	-10.92	-16.17	-10.56	-11.55	-7.19	-12.78	-6.81	-8.34
Cr	C	-9.05	-15.76	-10.72	-10.07	-4.82	-12.25	-6.93	-6.19
	D	-17.22	-19.98	-17.82	-17.41	-12.52	-16.32	-14.11	-13.14
	A	-9.69	-14.49	-11.96	-11.04	-8.45	-13.40	-10.82	-9.08
54	B	-10.12	-15.25	-8.56	-10.20	-8.83	-14.11	-7.35	-9.19
Fe	C	-7.92	-15.07	-8.51	-8.02	-6.42	-13.91	-7.30	-6.79
	D	-16.07	-18.99	-16.08	-15.32	-14.44	-17.74	-14.92	-13.98
	A	-10.84	-15.74	-13.70	-12.98	-8.46	-13.59	-11.31	-10.54
56	B	-11.32	-16.67	-9.99	-11.57	-8.92	-14.34	-7.53	-9.42
Fe	C	-9.02	-16.20	-10.25	-9.71	-6.37	-13.73	-7.69	-7.11
	D	-18.17	-21.09	-18.36	-17.73	-15.14	-18.58	-15.86	-14.91
	A	-11.82	-17.02	-15.44	-14.78	-8.43	-13.81	-11.78	-11.10
58	B	-12.33	-17.96	-11.72	-13.15	-8.91	-14.43	-7.97	-9.75
Fe	C	-9.97	-17.14	-12.20	-11.59	-6.29	-13.41	-8.33	-7.62
	D	-20.17	-23.26	-20.75	-20.22	-15.80	-19.43	-16.81	-15.87
	A	-12.95	-18.44	-17.08	-16.28	-8.40	-14.10	-12.16	-11.40
60	B	-13.31	-19.22	-13.48	-14.78	-8.87	-14.45	-8.47	-10.10
Fe	C	-10.92	-18.18	-14.09	-13.30	-6.20	-13.12	-8.94	-8.05
	D	-22.06	-25.65	-23.06	-22.44	-16.42	-20.38	-17.65	-16.64

Table 4.5: Contd...

Nucl	Int	Proton orbits f5/2	f7/2	p3/2	p1/2	Neutron orbits f5/2	f7/2	p3/2	p1/2
	A	-9.87	-14.72	-12.30	-11.49	-9.87	-14.72	-12.30	-11.49
56	B	-10.37	-15.61	-8.37	-10.38	-10.37	-15.61	-8.37	-10.38
Ni	C	-7.83	-15.23	-8.39	-7.97	-7.83	-15.23	-8.39	-7.97
	D	-17.01	-19.99	-16.69	-15.83	-17.01	-19.99	-16.69	-15.83
	A	-11.03	-15.98	-14.00	-13.35	-9.90	-14.92	-12.75	-12.09
58	B	-11.60	-17.09	-9.70	-11.66	-10.47	-15.88	-8.49	-10.57
Ni	C	-8.94	-16.39	-10.00	-9.53	-7.78	-15.09	-8.75	-8.26
	D	-19.14	-22.24	-18.84	-18.04	-17.72	-20.91	-17.53	-16.62
	A	-12.13	-17.14	-15.40	-14.57	-9.24	-14.37	-11.68	-10.89
60	B	-12.62	-18.37	-11.41	-13.22	-10.45	-15.96	-8.92	-10.90
Ni	C	-9.91	-17.36	-11.96	-11.39	-7.69	-14.77	-9.41	-8.80
	D	-21.13	-24.38	-21.30	-20.58	-18.35	-21.74	-18.56	-17.62
	A	-13.21	-18.75	-17.26	-16.51	-9.90	-15.47	-13.50	-12.84
62	B	-13.59	-19.64	-13.15	-14.81	-10.39	-15.98	-9.45	-11.28
Ni	C	-10.88	-18.40	-13.86	-13.12	-7.57	-14.45	-10.05	-9.26
	D	-22.97	-26.74	-23.65	-22.85	-18.91	-22.69	-19.48	-18.47
	A	-13.74	-19.56	-17.92	-17.06	-9.88	-15.65	-13.58	-12.86
63	B	-14.06	-20.30	-14.01	-15.55	-10.32	-16.00	-9.72	-11.45
Ni	C	-11.37	-18.99	-14.74	-13.87	-7.49	-14.31	-10.34	-9.44
	D	-23.82	-28.01	-24.78	-23.87	-19.12	-23.18	-19.90	-18.82
	A	-14.29	-20.39	-18.55	-17.58	-9.90	-15.85	-13.65	-12.87
64	B	-14.55	-20.95	-14.83	-16.32	-10.28	-16.02	-9.94	-11.62
Ni	C	-11.87	-19.62	-15.48	-14.50	-7.45	-14.23	-10.51	-9.53
	D	-24.71	-29.23	-25.98	-24.96	-19.37	-23.66	-20.38	-19.22
	A	-13.20	-18.96	-17.76	-17.07	-10.95	-16.70	-15.36	-14.75
64	B	-13.63	-19.77	-13.47	-15.14	-11.53	-17.31	-11.01	-12.77
Zn	C	-10.80	-18.08	-14.59	-13.73	-8.58	-15.40	-12.08	-11.22
	D	-23.57	-27.61	-24.69	-23.76	-20.87	-24.86	-21.91	-20.85
	A	-14.11	-20.62	-18.97	-18.08	-10.99	-17.11	-15.46	-14.72
66	B	-14.60	-21.05	-15.17	-16.67	-11.42	-17.31	-11.56	-13.17
Zn	C	-11.80	-19.36	-16.07	-14.98	-8.48	-15.22	-12.43	-11.39
	D	-25.27	-30.07	-26.99	-25.83	-21.30	-25.82	-22.84	-21.83
	A	-15.43	-22.37	-20.05	-18.90	-11.00	-17.58	-15.45	-14.55
68	B	-15.55	-22.32	-16.91	-18.19	-11.26	-17.31	-12.13	-13.57
Zn	C	-12.84	-20.77	-17.37	-16.02	-8.38	-15.13	-12.64	-11.41
	D	-26.97	-32.42	-29.59	-28.13	-21.67	-26.72	-23.99	-22.57
	A	-15.48	-22.68	-20.36	-19.20	-12.13	-18.98	-17.03	-16.07
70	B	-15.55	-22.35	-17.37	-18.58	-12.31	-18.55	-13.87	-15.22
Ge	C	-12.77	-20.57	-17.79	-16.31	-9.39	-16.25	-14.36	-13.01
	D	-27.53	-33.30	-30.61	-28.98	-23.55	-28.91	-26.53	-24.98

A:KB3P-1H B:MWH C:MWH2 D:KB10

Table 4.6: Coulomb corrected (-Ej) for proton orbits (f-p shell)

Nucl	Int	f5/2	f7/2	p3/2	p1/2
	A	2.07	-3.33	-.58	.85
46	B	2.03	-3.59	.70	.88
Ti	C	3.03	-3.59	.70	1.88
	D	-1.02	-5.04	-2.34	-1.22
	A	.31	-4.77	-1.93	-.67
48	B	.14	-5.12	-.19	-.43
Ti	C	1.36	-5.12	-.17	.81
	D	-3.73	-7.13	-4.45	-3.61
	A	-1.18	-6.12	-3.55	-2.50
50	B	-1.57	-6.59	-1.35	-1.86
Ti	C	-.24	-6.58	-1.23	-.43
	D	-6.15	-9.12	-6.86	-6.83
	A	.55	-4.39	-1.59	-.41
50	B	.33	-4.88	.77	-.13
Cr	C	2.02	-4.85	.82	1.59
	D	-4.11	-7.38	-4.70	-3.84
	A	-.92	-5.76	-3.21	-2.22
52	B	-1.29	-6.37	-.44	-1.52
Cr	C	.47	-6.28	-.36	.28
	D	-6.60	-9.48	-6.95	-6.30
	A	-9.72	-14.61	-12.59	-11.81
54	B	-10.07	-15.32	-9.71	-10.70
Cr	C	-8.20	-14.91	-9.87	-9.22
	D	-16.37	-19.13	-16.97	-16.56
	A	-.63	-5.43	-2.90	-1.98
54	B	-1.06	-6.19	.50	-1.14
Fe	C	1.14	-6.01	.55	1.04
	D	-7.01	-9.93	-7.02	-6.26
	A	-1.86	-6.76	-4.72	-4.00
56	B	-2.34	-7.69	-1.01	-2.59
Fe	C	-.04	-7.22	-1.27	-.73
	D	-9.19	-12.11	-9.38	-8.75
	A	-3.02	-8.12	-6.54	-5.88
58	B	-3.43	-9.06	-2.82	-4.25
Fe	C	-1.07	-8.24	-3.30	-2.69
	D	-11.27	-14.36	-11.85	-11.32
	A	-4.13	-9.62	-8.26	-7.46
60	B	-4.49	-10.40	-4.66	-5.96
Fe	C	-2.10	-9.36	-5.27	-4.48
	D	-13.24	-16.83	-14.24	-13.62

Table 4.6: Contd....

Nucl	Int	f5/2	f7/2	p3/2	p1/2
	A	-.25	-5.10	-2.68	-1.87
56	B	-.75	-5.99	1.25	-.76
Ni	C	1.79	-5.61	1.23	1.65
	D	-7.39	-10.37	-7.07	-6.21
	A	-1.49	-6.44	-4.46	-3.81
58	B	-2.06	-7.55	-.16	-2.12
Ni	C	.60	-6.85	-.46	.01
	D	-9.60	-12.70	-9.30	-8.50
	A	-2.67	-7.68	-5.94	-5.11
60	B	-3.16	-8.91	-1.95	-3.76
Ni	C	-.45	-7.90	-2.50	-1.93
	D	-11.67	-14.92	-11.84	-11.12
	A	-3.83	-9.37	-7.88	-7.13
62	B	-4.21	-10.26	-3.77	-5.43
Ni	C	-1.50	-9.02	-4.48	-3.74
	D	-13.59	-17.36	-14.27	-13.47
	A	-4.40	-10.22	-8.58	-7.72
63	B	-4.72	-10.96	-4.67	-6.21
Ni	C	-2.03	-9.65	-5.40	-4.53
	D	-14.48	-18.67	-15.44	-14.53
	A	-4.98	-11.08	-9.24	-8.27
64	B	-5.24	-11.64	-5.52	-7.01
Ni	C	-2.56	-10.31	-6.17	-5.19
	D	-15.40	-19.92	-16.67	-15.65
	A	-3.27	-9.03	-7.83	-7.14
64	B	-3.70	-9.84	-3.54	-5.21
Zn	C	-.87	-8.15	-4.66	-3.80
	D	-13.64	-17.68	-14.76	-13.83
	A	-4.26	-10.77	-9.12	-8.23
66	B	-4.75	-11.20	-5.32	-6.82
Zn	C	-1.95	-9.51	-6.22	-5.13
	D	-15.42	-20.22	-17.14	-15.98
	A	-5.65	-12.59	-10.27	-9.12
68	B	-5.77	-12.54	-7.13	-8.41
Zn	C	-3.06	-10.99	-7.59	-6.24
	D	-17.19	-22.64	-19.81	-18.35
	A	-5.17	-12.37	-10.05	-8.89
70	B	-5.24	-12.04	-7.06	-8.27
Ge	C	-2.46	-10.26	-7.48	-6.00
	D	-17.22	-22.99	-20.30	-18.67

A:KB3P-1H, B:MWH2, C:MWH, D:KB10

Table 4.7: Experimental values for proton energy positions

Nucl	f5/2	f7/2	p3/2	p1/2
^{46}Ti	2.07±.01	$5.37^{+.17}_{-.35}$	2.53±.24	0.73±.01
^{48}Ti	2.05	6.99±.36	3.95±.54	1.88±.45
^{50}Ti		8.67±.80	5.10±.80	
^{50}Cr	1.97	$6.54^{+.32}_{-.40}$	$2.14^{+.55}_{-.40}$	2.55
^{52}Cr		8.21±1.0	2.87±1.0	
^{54}Cr		9.32±1.0	4.92±1.0	
^{54}Fe		7.62±.80	2.61±.80	
^{56}Fe	3.2±.70	8.89±.35	4.54±.33	4.52
^{58}Fe		10.50±.80	5.85±.80	

Table 4.8: 1f7/2-2p3/2 energy spacing for protons and neutrons

		proton energy spacing					neutron energy spacing			
NP	NN	MWH2	MWH	3P-1H	KB10	EXPT	MWH2	MWH	3P-1H	KB10
22	24	4.29	4.29	2.75	2.70	2.8	4.35	4.35	2.46	2.40
	26	4.95	4.93	2.84	2.68	3.0	5.07	5.06	2.34	2.25
	28	5.85	5.24	2.57	2.26	3.6	5.56	5.52	2.23	2.00
24	26	5.67	5.65	2.80	2.38	4.4	5.73	5.71	2.65	2.53
	28	5.92	5.93	2.55	2.52	5.3	6.07	6.12	2.51	2.41
	30	5.02	5.61	2.02	2.16	4.4	5.32	5.97	2.28	2.21
26	28	6.56	6.69	2.53	2.91	5.0	6.61	6.76	2.58	2.82
	30	6.35	6.68	2.04	2.73	4.4	6.04	6.81	2.28	2.70
	32	4.94	6.24	1.58	2.51	4.7	5.08	6.46	2.03	2.62
	34	4.09	5.74	1.36	2.59		4.18	5.98	1.94	2.73
28	28	6.84	7.24	2.42	3.30		6.84	7.24	2.42	3.30
	30	6.39	7.39	1.98	3.40		6.34	7.39	2.17	3.38
	32	5.40	6.96	1.74	3.08		5.36	7.04	2.69	3.18
	34	4.54	6.49	1.49	3.09		4.40	6.53	1.93	3.21
	35	4.25	6.29	1.64	3.23		3.97	6.28	2.07	3.28
	36	4.14	6.12	1.84	3.25		3.72	6.08	2.20	3.28
30	34	3.49	6.30	1.20	2.92		3.32	6.30	1.34	2.95
	36	3.29	5.88	1.65	3.08		2.79	5.76	1.65	2.98
	38	3.40	5.41	2.32	2.83		2.49	5.18	2.13	2.73
32	38	2.78	4.98	2.32	2.69		1.89	4.68	1.95	2.38

Figures 4.3a-d: Proton and neutron effective single particle energies for various nuclei using four effective interactions namely KB3p-1h, MWH, MWH2 and KB10, alongwith the experimental results (for protons) from reference no. 41. Energy values for isotopes are connected via lines/dashes for different interactions which are identified through different symbols.

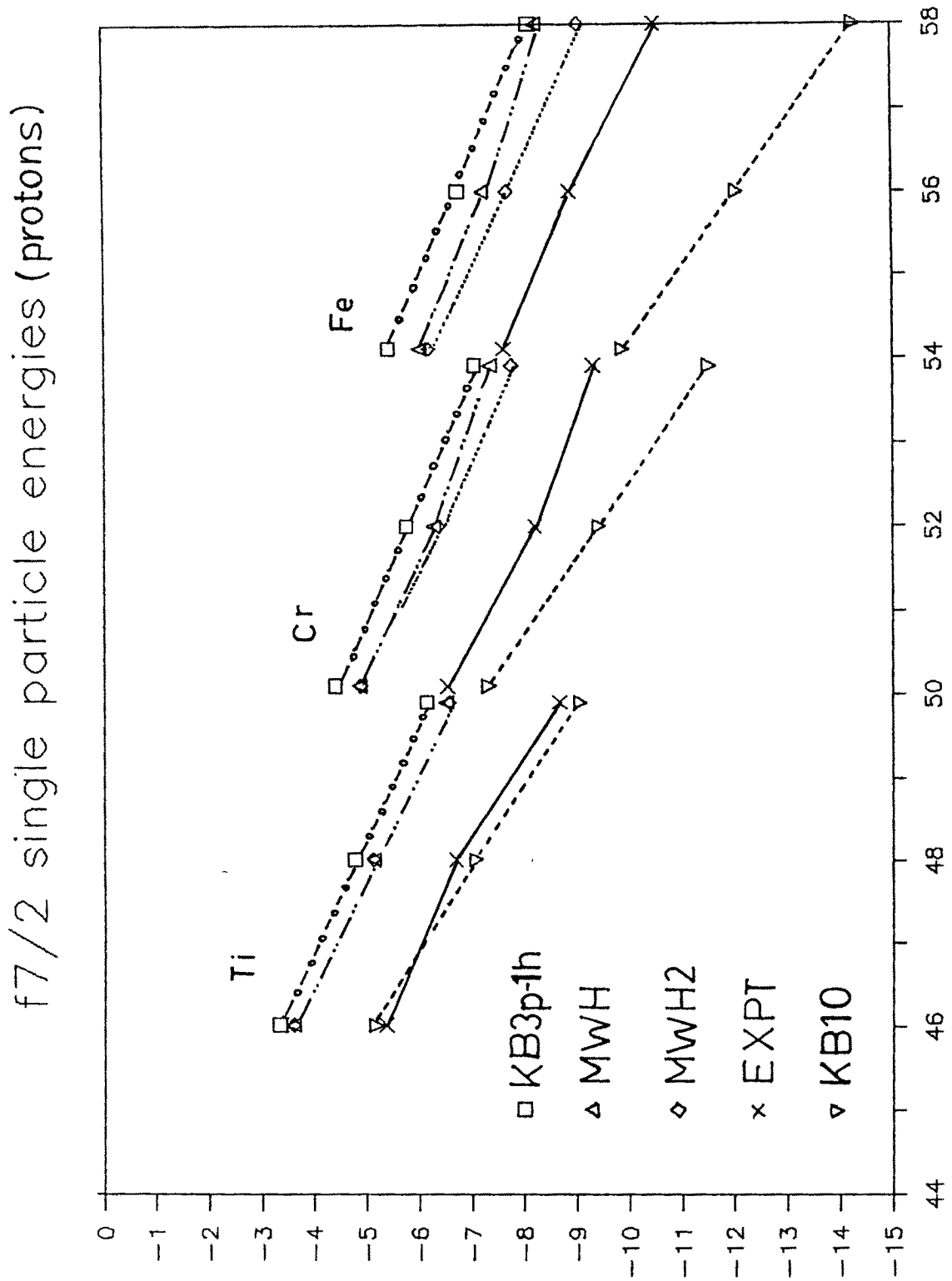
f7/2 single particle energies (protons)
Ti
Cr
Fe
KB3p-1h
MWH
MWH2
EXPT
KB10
MASS NUMBER
0
−1
−2
−3
−4
−5
−6
−7
−8
−9
−10
−11
−12
−13
−14
−15
44
46
48
50
52
54
56
58

Fig. 4.3a

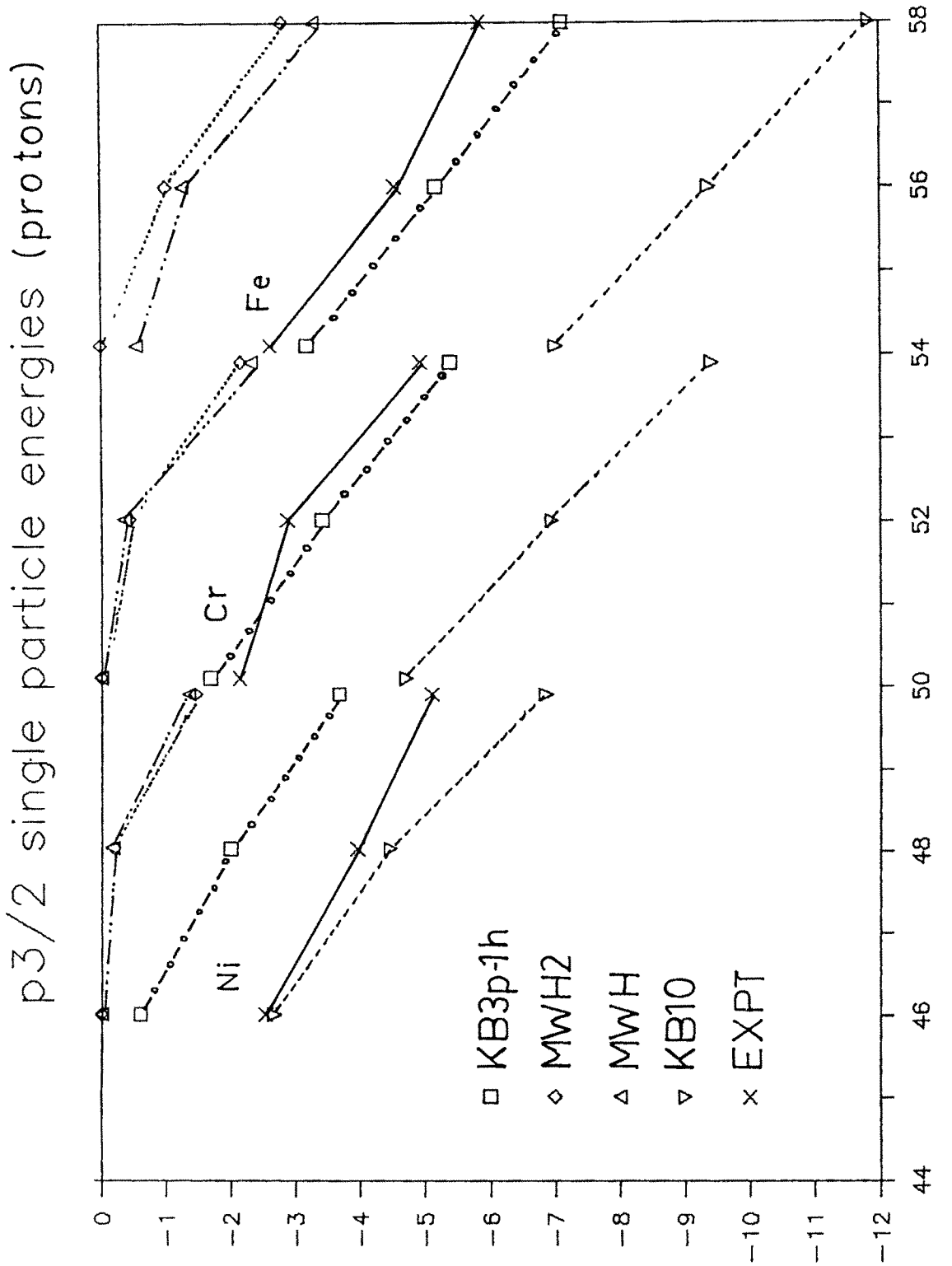
p3/2 single particle energies (protons)
Ni
Cr
Fe
KB3p-1h
MWH2
MWH
KB10
EXPT
MASS NUMBER
0
-1
-2
-3
-4
-5
-6
-7
-8
-9
-10
-11
-12
44
46
48
50
52
54
56
58

Fig. 4.3b

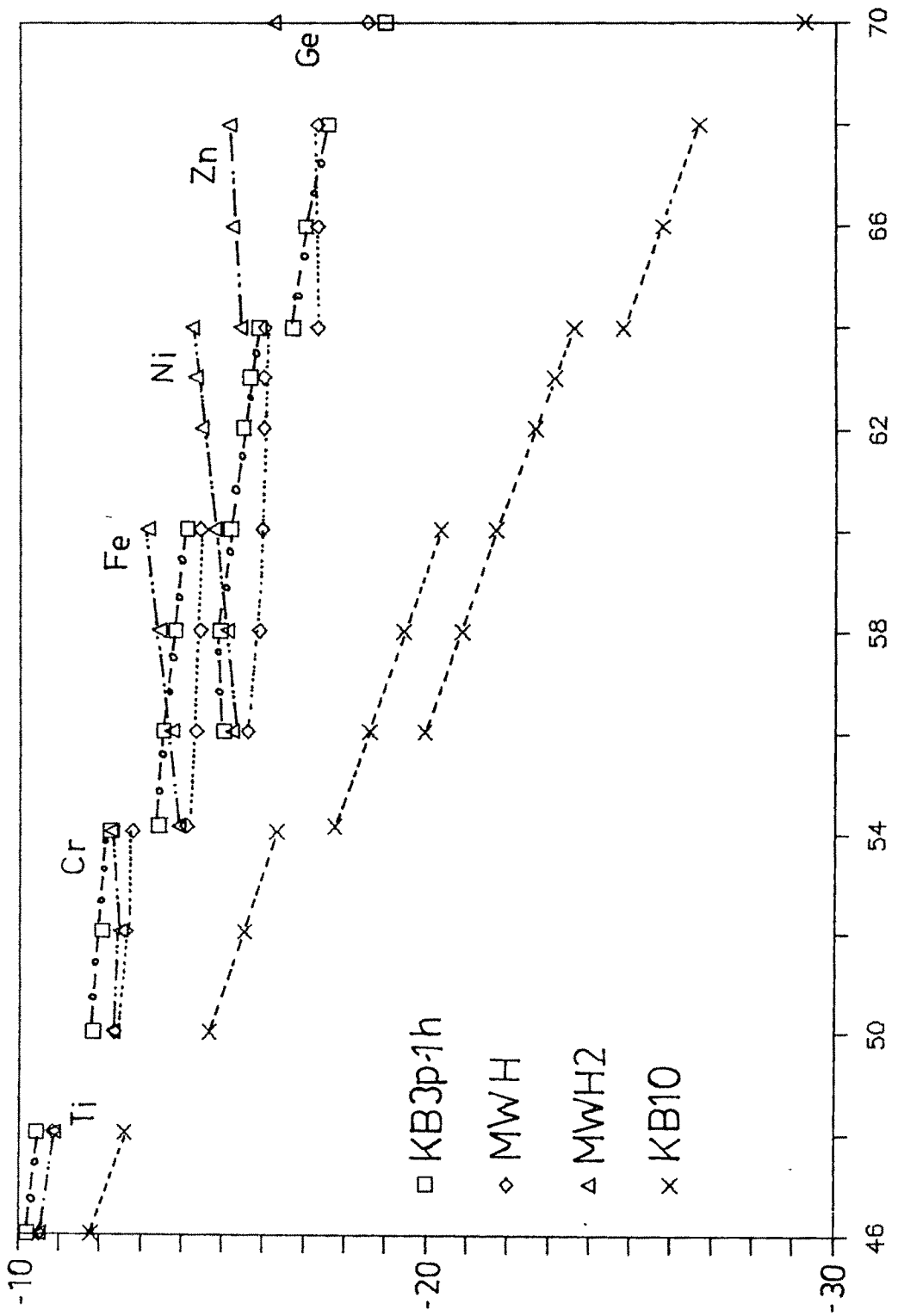
f7/2 neutron single particle energy
-10
-20
-30
46
50
54
58
62
66
70
MASS NUMBER
Ti
Cr
Fe
Ni
Zn
Ge
KB3p-1h
MWH
MWH2
KB10

Fig. 4.3c

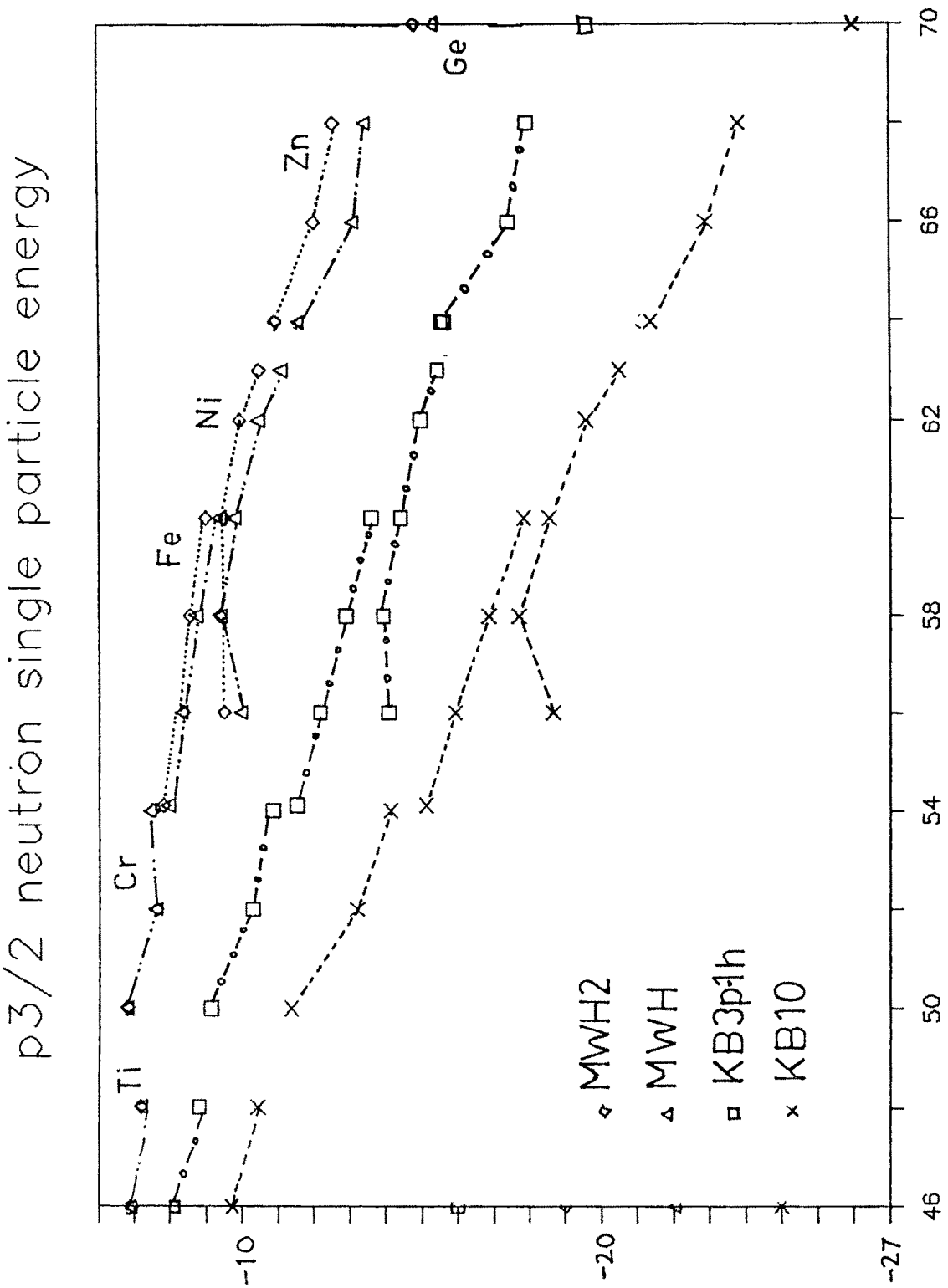
p3/2 neutron single particle energy
Ti
Cr
Fe
Ni
Zn
Ge
MWH2
MWH
KB3p1h
KB10
-10
-20
-27
46
50
54
58
62
66
70
MASS NUMBER

Fig. 4.3d

Discussion

Though experimental values of ground state occupancies for f-p shell nuclei have been reported by a number of people, there is unfortunately not much data on single particle energies, providing limited source for comparison with theoretical predictions. There are large uncertainities involved in the experimental results, making it difficult to judge which effective interaction gives the best fit.

Fig.4.3a which shows the proton energy values for different effective interactions, shows a considerable difference between the effective single particle energies between KB10 and other effective interactions. The discrepancy in occupancy predictions as well as induced single particle energies of the four effective interactions are reflected in the effective single particle energy plot. Values predicted by MWH and MWH2 interactions lie very close to each other, which is expected since the interactions themselves do not differ much from each other. All experimental results lie within the range of the theoretical predictions, but cannot be distinctly said to lie extremely close to any of the theoretical results, as was the case with s-d shell nuclei. One reason for this could be that whereas extensive experimental work has been carried out for s-d shell nuclei, there is much less stripping and pickup reaction data in the f-p shell range. Since the calculation for effective single particle energy requires joint analysis of stripping and pickup reaction data, the input experimental data is itself scarce to give satisfactory single particle energy values. On the average, the MWH interaction is closer to the experimental predictions for $f_{7/2}$ orbit energies. For the $p_{3/2}$ orbit, the KB3p-1h interaction gives a better fit.

The experimental trend is reproduced by all the four effective interactions almost throughout the spectrum.

An interesting behaviour is observed at shell closure for the nuclei, by looking at the proton energy gap between $f_{7/2}$ and $p_{3/2}$ orbits. These values are displayed in Table 4.8. Experimentally, a clearcut maxima is exhibited as the neutron number approaches 28 for a set of isotopes of any nucleus, highlighting shell closure at magic number N = 28. This tendency is repeated for isotopes of all nuclei. It is naturally desirable to check for this behaviour in theoretical results too. It turns out that for theoretical results, such a behaviour is seen throughout the span of nuclei for the MWH2 interaction (where the isotopes of different nuclei having N = 28 do not even once fail to show up a maximum). For the KB3p-1h and MWH effective interactions, there are a few cases in the low-mass region where discrepancies from this behaviour are observed. The KB10 interaction clearly does not exhibit such a behaviour as the energy gap is distinctly larger for the lowest mass isotope of any nucleus. There is a general trend of the energy gap to reduce with increase in neutron no., as can be seen for almost all nuclei for all the effective interactions.

Just as increase in the $f_{7/2}$-$p_{3/2}$ energy gap is observed as the neutron number approaches 28, a similar peak is expected at proton number Z = 28. Interestingly, all isotopes of Fe (Z = 28) do display a maxima in the $f_{7/2}$-$p_{3/2}$ energy gap with respect to other nuclei. This is true for almost all interactions.

No experimental results are available for neutron effective single particle energy. Among the theoretical results, again the MWH2 effective interaction

results for $f_{7/2}$-$p_{3/2}$ energy gap display a peak at N = 28 and Z = 28, throughout the range of nuclei. In fact, all trends for neutron effective single particle energies are similar to the proton effective single particle energies.

(c) Upper f-p-g shell

The upper f-p-g shell covers the space of four orbits, namely the $p_{3/2}$, $f_{5/2}$, $p_{1/2}$ and $g_{9/2}$ orbits above the ^{56}Ni core. The bare Kuo-Brown effective interaction based on the Hamada-Johnston potential was renormalised in several stages to obtain a series of effective interactions. These include renormalisation effect of two-particle - two-hole, three-particle - one-hole, four-particle - two-hole excitations from the $f_{7/2}$ orbital. Two of the effective interactions considered here are:

1 the fully renormalised Kuo-Brown effective interaction, in which the bare two-nucleon interaction is renormalised for 3p-1h+2p+4p-2h excitations of the $f_{7/2}$ orbit and

2 the Bhatt-Ahalpara effective interaction which was derived from the fully renormalised Kuo-Brown interaction /42/. The following modifications were done empirically:

(i) The $\langle g^2_{9/2}|V|g^2_{9/2}\rangle^{JT}$ matrix elements were changed using Hartree-Fock calculations so as to reproduce ^{90}Zr and ^{92}Mo spectra.

(ii) The centroid of $\langle g_{9/2}\ p_{1/2}|V|g_{9/2}p_{1/2}\rangle^{JT}$ matrix elements was raised by .01 MeV to reproduce the separation of the $g_{9/2}$ and $p_{1/2}$ single particle states in ^{89}V nucleus.

(iii) The centroid of $\langle g_{9/2}f_{5/2}|V|g_{9/2}f_{5/2}\rangle^{JT}$ and $\langle g_{9/2}p_{3/2}|V|g_{9/2}p_{3/2}\rangle^{JT}$ was also raised by 0.05 MeV.

(iv) The $p_{3/2}$ orbit self-interaction was made slightly repulsive by adding 0.16 MeV to all matrix elements of the type $\langle p_{3/2}{}^2|V|p_{3/2}{}^2\rangle^{JT}$.

(v) The $f_{5/2}$ orbit self - interaction was made attractive by subtracting 0.05 MeV from $\langle f_{5/2}{}^2|V|f_{5/2}{}^2\rangle^{JT}$ matrix elements.

The single particle energies for the $p_{3/2}$, $f_{5/2}$ and $p_{1/2}$ orbits are taken from the spectrum of ^{57}Ni, the values being 0.0, 0.78 and 1.08 MeV for the three orbits respectively. The $g_{9/2}$ single particle energy is fixed at 3 MeV.

Ground state occupancies, single nucleon transfer strength centroids and widths (both for particle removal and addition) have been calculated for the two interactions using proton-neutron configuration space. It is usually found that widths of different configurations do not differ much from each other, fluctuating around a mean average width by maximum 1 MeV. Therefore, we have performed all calculations in the upper f-p shell assuming a constant configuration width. This is done in order to save a lot of computation time involved in width calculation.

Table 4.9 contains six columns which display the following:

(i) centroid of particle removal strength (EMS) using bivariate gaussian approach, (ii) centroid for particle addition strength (EP1)†, which is calculated from EMS using the identity given by equation (7), (iii) centroid of particle addition strength (EP2)† using bivariate gaussian approach, (iv)width of particle removal strength (SIG), (v) width of

† Values exceeding 100 Mev are replaced by the figure 99.9.

particle addition strength (SIG+) and (vi) effective single particle energy (-E_j). Results for the Bhatt-Ahalpara interaction (BA) and the fully renormalised Kuo-Brown interaction (KB) are displayed beside each other. There are eight rows corresponding to the four orbits marked by p3, f5, p1 and g9. Table 4.9a give proton results, while the neutron results are given in Table 4.9b.

We have not been able to gather enough experimental data again due to scarcity of experiments in this region. Table 4.10 gives the ground-state occupancies for the pickup or stripping reactions for protons and neutrons /43,44/. Experimental values, obtained using French - Macfarlane sum-rules are normalized for the f-p-g shell wherever possible. They are plotted against the theoretical occupancies in Figs.4.4a-d. Table4.11 gives experimental centroids for proton and neutron stripping and pickup strengths.

Discussion

Ground state occupancies have been calculated in the past for a number of nuclei in the upper f-p-g shell /45,46/. The interactions used were different, and different approximations were involved for the calculation of binding energies and occupancies. A major approximation involved in this work is the assumption of a constant configuration width. The error in binding energy due to this approximation is less than 2 MeV, due to which the error in occupancy and centroid calculations turns out to be negligible. From Figs.4.4a-d, it is observed that the occupancy predictions of the two effective interactions vary from each other, except for the $g_{9/2}$ orbit which shows nearly a constant occupation for isotopes of a particular nucleus. When

Table 4. 9a:Centroids and widths for proton removal(-) and addition(+) strengths for upper f-p-g-shell nuclei.

Nucl		EMS		SIG-		EP1		EP2		SIG+		-Ej	
		BA	KB	BA	KB	BA	KB	BA	KB	BA	KB	BA	KB
	p3	8.1	8.5	1.6	1.6	-1.8	-2.4	-3.3	-4.1	2.2	2.2	4.0	4.9
64	f5	7.5	7.0	2.0	1.9	-1.5	-1.5	-.3	-1.8	2.4	2.4	1.7	1.6
Zn	p1	7.9	7.9	1.8	1.7	-2.4	-3.1	-2.0	-2.3	2.5	2.4	3.4	3.7
	g9	5.4	4.7	1.9	1.6	.7	.3	1.9	.9	2.3	2.1	-.7	-.3
	p3	9.3	9.9	1.6	1.6	-2.8	-3.0	-4.7	-5.5	2.2	2.2	5.0	5.9
66	f5	8.9	8.6	1.9	1.9	-2.6	-2.7	-1.8	-1.6	2.4	2.4	2.9	2.8
Zn	p1	9.2	9.4	1.8	1.7	-3.3	-4.1	-3.3	-3.5	2.5	2.4	4.3	4.6
	g9	6.5	6.1	1.8	1.6	-.3	-.8	.5	-.6	2.3	2.0	.3	.8
	p3	10.1	11.0	1.5	1.5	-3.7	-3.8	-5.9	-6.7	2.0	2.0	5.8	6.8
68	f5	9.9	10.0	1.8	1.8	-3.7	-3.9	-3.5	-3.2	2.3	2.3	4.1	4.0
Zn	p1	10.0	10.5	1.7	1.7	-4.1	-4.9	-4.1	-4.7	2.3	2.3	5.0	5.4
	g9	7.3	7.3	1.7	1.5	-1.2	-1.9	-.9	-2.1	2.2	1.9	1.3	1.9
	p3	8.1	8.5	1.9	1.9	-.3	-.3	-2.9	-3.9	2.4	2.4	4.1	5.1
65	f5	7.2	6.6	2.3	2.2	-1.2	-1.4	.2	.2	2.6	2.5	1.6	1.5
Ga	p1	7.9	7.8	2.0	2.0	-1.5	-2.6	-1.6	-2.1	2.7	2.6	3.4	3.8
	g9	5.0	4.2	2.2	1.9	.7	.3	2.2	1.2	2.5	2.2	-.6	-.2
	p3	9.1	9.8	1.8	1.8	-1.4	-.9	-4.3	-5.3	2.3	2.3	5.0	6.1
67	f5	8.4	8.1	2.2	2.2	-2.3	-2.5	-1.3	-1.2	2.5	2.5	2.8	2.7
Ga	p1	9.0	9.1	2.0	2.0	-2.5	-3.5	-2.9	-3.3	2.7	2.5	4.3	4.7
	g9	6.0	5.5	2.1	1.8	-.3	-.8	-.6	-.3	2.5	2.1	.3	.8
	p3	9.9	10.8	1.7	1.7	-2.6	-1.6	-5.5	-6.5	2.2	2.2	5.8	6.9
69	f5	9.5	9.4	2.1	2.1	-3.3	-3.7	-3.0	-2.7	2.4	2.4	4.1	3.9
Ga	p1	9.8	10.1	2.0	1.9	-3.5	-4.5	-4.0	-4.4	2.5	2.5	5.0	5.6
	g9	6.8	6.7	2.0	1.7	-1.2	-2.0	-.6	-1.8	2.3	2.0	1.3	2.0
	p3	10.4	11.5	1.6	1.6	-3.9	-3.0	-6.6	-7.5	2.0	2.0	6.5	7.7
71	f5	10.4	10.6	1.9	1.9	-4.3	-4.8	-4.7	-4.4	2.3	2.2	5.3	5.3
Ga	p1	10.3	10.9	1.8	1.8	-4.5	-5.4	-5.0	-5.5	2.3	2.3	5.6	6.3
	g9	7.4	7.7	1.8	1.5	-2.2	-3.1	-2.0	-3.3	2.2	1.8	2.2	3.1

Table 4. 9a: Contd...

Nucl		EMS		SIG-		EP1		EP2		SIG+		-Ej	
		BA	KB	BA	KB	BA	KB	BA	KB	BA	KB	BA	KB
	p3	10.1	11.1	1.9	1.9	-.2	4.1	-5.3	-6.3	2.3	2.3	5.9	7.2
70	f5	9.4	9.2	2.3	2.2	-3.0	-3.5	-2.2	-2.5	2.5	2.5	3.9	3.8
Ge	p1	10.0	10.4	2.2	2.1	-2.4	-3.6	-3.7	-4.2	2.7	2.6	5.2	5.8
	g9	6.8	6.5	2.2	1.8	-1.2	-2.0	.0	-1.5	2.4	2.1	1.2	2.0
	p3	10.6	11.8	1.7	1.8	-2.2	1.8	-6.3	-7.3	2.1	2.2	6.6	7.9
72	f5	10.3	10.3	2.1	2.1	-3.9	-4.6	-4.2	-3.9	2.4	2.3	5.2	5.1
Ge	p1	10.4	11.0	2.0	2.0	-3.8	-4.8	-4.7	-5.3	2.5	2.4	5.7	6.5
	g9	7.3	7.4	1.9	1.7	-2.2	-3.1	-1.6	-3.0	2.2	1.9	2.2	3.1
	p3	10.9	12.2	1.5	1.5	-4.2	-1.5	-7.3	-8.3	1.9	2.0	7.3	8.5
74	f5	10.9	11.3	1.8	1.9	-4.8	-5.7	-6.0	-5.7	2.1	2.1	6.6	6.5
Ge	p1	10.6	11.4	1.8	1.8	-5.1	-5.9	-5.7	-6.3	2.2	2.2	6.3	7.1
	g9	7.6	8.3	1.7	1.5	-3.1	-4.3	-3.0	-4.6	2.0	1.7	3.1	4.3
	p3	11.1	12.4	1.3	1.3	-6.1	-4.9	-8.4	-8.9	1.6	1.8	7.9	9.0
76	f5	11.5	12.1	1.5	1.6	-5.8	-6.7	-7.8	-7.6	1.8	1.8	7.9	7.9
Ge	p1	10.7	11.7	1.5	1.5	-6.2	-6.9	-6.8	-7.3	1.9	2.0	6.8	7.6
	g9	7.7	9.1	1.4	1.2	-3.9	-5.5	-4.2	-6.2	1.6	1.4	3.9	5.6

Table 4. 9b:Centroids and widths for neutron removal(-) and addition(+) strengths for upper f-p-g shell nuclei.

Nucl		EMS		SIG-		EP1		EP2		SIG+		-Ej	
		BA	KB	BA	KB	BA	KB	BA	KB	BA	KB	BA	KB
	p3	6.7	6.9	2.4	2.3	22.8	45.7	2.5	4.3	2.8	2.6	1.8	2.6
64	f5	5.1	4.4	2.5	2.4	1.9	1.4	4.4	4.1	2.7	2.6	-.5	-.6
Zn	p1	6.0	5.6	2.4	2.3	6.8	5.4	3.4	2.6	2.9	2.7	1.0	1.3
	g9	3.8	3.1	2.5	2.3	2.3	1.9	6.1	5.0	2.7	2.5	-2.2	-1.8
	p3	7.1	7.6	2.6	2.5	48.0	99.9	3.6	2.6	2.9	2.7	1.8	2.7
66	f5	5.3	4.7	2.8	2.7	3.9	2.6	5.2	4.5	2.8	2.7	-.5	-.5
Zn	p1	6.3	6.2	2.6	2.5	13.5	15.2	4.7	3.8	3.0	2.8	.8	1.2
	g9	3.9	3.5	2.8	2.6	2.5	2.0	6.7	5.6	2.8	2.7	-2.1	-1.5
	p3	7.1	7.9	2.7	2.6	69.0	99.9	4.5	3.7	2.9	2.8	1.6	2.6
68	f5	5.5	5.2	2.9	2.8	7.8	4.5	5.8	5.6	2.8	2.7	-.3	-.3
Zn	p1	6.3	6.5	2.8	2.7	17.1	22.1	5.7	4.9	3.0	2.8	.5	1.1
	g9	4.1	4.1	2.8	2.7	2.9	2.3	7.3	6.0	2.9	2.7	-2.0	-1.1
	p3	6.9	7.3	2.4	2.4	15.9	28.7	1.1	.1	2.8	2.7	2.4	3.4
65	f5	5.3	4.5	2.7	2.6	1.5	.9	3.5	3.2	2.8	2.7	.0	-.1
Ga	p1	6.4	6.1	2.5	2.5	5.7	4.2	2.3	1.4	3.0	2.8	1.6	2.0
	g9	3.7	2.9	2.6	2.4	2.0	1.5	5.2	4.0	2.8	2.6	-1.8	-1.4
	p3	7.2	7.8	2.7	2.6	33.9	79.4	2.3	1.0	2.9	2.8	2.4	3.4
67	f5	5.4	4.8	2.9	2.8	3.2	1.9	4.3	4.0	2.9	2.8	.0	-.1
Ga	p1	6.6	6.5	2.8	2.7	11.8	12.8	3.5	2.5	3.1	2.9	1.5	2.0
	g9	3.8	3.3	2.8	2.6	2.2	1.5	5.8	4.4	2.9	2.7	-1.7	-1.0
	p3	7.1	8.0	2.8	2.7	49.3	99.9	3.3	3.1	2.9	2.9	2.2	3.3
69	f5	5.6	5.2	3.0	2.9	6.5	3.5	4.8	4.6	2.9	2.8	.2	.2
Ga	p1	6.5	6.8	2.9	2.8	15.3	20.0	4.6	3.6	3.1	3.0	1.2	1.9
	g9	3.9	3.8	2.9	2.7	2.5	1.8	6.4	4.8	3.0	2.7	-1.6	-.7
	p3	6.7	7.9	2.8	2.7	62.4	99.9	3.9	3.1	2.8	2.9	2.0	3.2
71	f5	5.6	5.5	3.0	3.0	13.4	5.9	5.1	4.9	2.9	2.8	.4	.5
Ga	p1	6.0	6.7	3.0	2.8	16.7	21.5	5.4	4.5	3.0	2.9	.9	1.7
	g9	3.8	4.2	3.0	2.8	3.1	2.4	6.8	5.0	2.9	2.6	-1.5	-.3

Table 4. 9b: Contd...

Nucl		EMS		SIG-		EP1		EP2		SIG+		-Ej	
		AL	BA	AL	BA	AL	BA	AL	BA	AL	BA	AL	BA
	p3	7.7	8.7	2.8	2.7	56.7	99.9	2.7	1.0	3.0	2.9	2.9	4.2
70	f5	6.0	5.6	3.1	3.0	5.7	2.8	4.9	4.1	3.0	2.9	.6	.6
Ge	p1	7.2	7.6	2.9	2.9	19.5	27.4	4.2	2.7	3.2	3.0	1.9	2.7
	g9	4.2	3.9	3.0	2.7	2.1	1.4	6.3	4.2	3.0	2.7	-1.2	-.3
	p3	7.2	8.5	2.9	2.8	66.9	99.9	3.2	2.0	2.9	2.9	2.6	4.0
72	f5	6.0	5.8	3.1	3.0	12.3	5.0	4.7	4.4	2.9	2.8	.8	.9
Ge	p1	6.7	7.4	3.0	2.9	19.6	29.3	4.8	3.7	3.1	3.0	1.5	2.5
	g9	4.0	4.2	3.0	2.8	2.6	1.8	6.3	4.4	2.9	2.7	-1.1	.1
	p3	6.5	8.0	2.8	2.8	83.4	99.9	3.7	3.1	2.7	2.8	2.4	3.8
74	f5	5.8	6.0	3.1	3.0	28.6	8.5	4.8	4.6	2.8	2.7	1.1	1.2
Ge	p1	5.9	7.0	3.0	2.9	20.1	22.5	5.3	4.5	2.9	2.9	1.2	2.3
	g9	3.6	4.4	2.9	2.8	3.3	2.6	6.6	4.4	2.8	2.5	-1.0	.5
	p3	5.6	7.2	2.7	2.7	99.9	62.5	3.9	3.4	2.4	2.4	2.2	3.4
76	f5	5.4	6.0	2.9	2.9	92.7	15.1	4.7	4.4	2.5	2.5	1.5	1.8
Ge	p1	4.8	6.3	2.9	2.8	25.1	12.3	5.5	5.0	2.6	2.6	.9	2.0
	g9	2.8	4.4	2.8	2.6	4.3	3.8	6.7	4.2	2.5	2.3	-1.0	1.0

Table 4.10: Ground state proton and neutron occpuancies for f-p-g shell nuclei.

Nucl	Int	Proton occupancy				Neutron occupancy			
		p3	f5	p1	g9	p3	f5	p1	g9
64 Zn	BA	1.40	.22	.37	.01	3.34	1.20	1.22	.23
	KB	1.67	.08	.24	.01	3.68	.85	1.21	.26
	R21						1.77		1.34
66 Zn	BA	1.36	.29	.34	.01	3.61	2.22	1.45	.72
	KB	1.68	.09	.22	.01	3.85	1.68	1.53	.93
	R21						3.02		1.16
68 Zn	BA	1.27	.44	.28	.01	3.71	3.37	1.51	1.41
	KB	1.66	.14	.19	.01	3.89	2.58	1.62	1.91
	R21						4.03		0.83
65 Ga	BA	1.93	.43	.60	.04	3.21	1.26	1.22	.31
	KB	2.31	.20	.46	.03	3.57	.88	1.20	.35
67 Ga	BA	1.88	.52	.56	.04	3.53	2.22	1.44	.81
	KB	2.33	.21	.43	.03	3.80	1.65	1.52	1.03
69 Ga	BA	1.76	.72	.48	.04	3.65	3.32	1.51	1.51
	KB	2.31	.28	.38	.03	3.86	2.50	1.63	2.01
	R22	2.54*	.38						
71 Ga	BA	1.58	1.00	.38	.04	3.73	4.36	1.54	2.37
	KB	2.20	.43	.33	.04	3.87	3.33	1.64	3.16
	R22	2.75*	.25						
70 Ge	BA	2.33	.87	.73	.07	3.70	3.24	1.60	1.46
	KB	2.96	.35	.63	.06	3.89	2.41	1.72	1.97
	R22	2.36	1.24	.59	.25				
72 Ge	BA	2.11	1.24	.58	.07	3.75	4.31	1.61	2.32
	KB	2.86	.52	.56	.07	3.90	3.24	1.73	3.12
	R22	2.35	1.34	.43	.25				
74 Ge	BA	1.83	1.68	.43	.06	3.82	5.19	1.64	3.35
	KB	2.64	.84	.45	.08	3.87	4.04	1.68	4.41
	R22	1.44	2.20	.43	.34				
76 Ge	BA	1.50	2.17	.30	.03	3.90	5.76	1.73	4.60
	KB	2.19	1.42	.31	.08	3.79	4.79	1.53	5.89
	R22	1.29	2.41	.40	.25				

* The value corresponds to l=1 occupancy

Table 4.11: Experimental centroids for single nucleon transfer reactions on Zn and Ge isotopes.

Reaction	p3/2	p1/2	f5/2	g9/2
$^{64}Zn(d,n)^{65}Ga$	$\geq$ 0.20	$\geq$ 0.53	0.05	> 2.5
$^{66}Zn(d,n)^{67}Ga$	0.19	$\geq$ 0.49	0.53	> 2.5
$^{68}Zn(d,n)^{69}Ga$	0.14	$\geq$ 0.61	0.76	> 2.5
$^{70}Ge(d,^{3}He)^{69}Ga$	0.33	0.41	0.62	1.97
$^{72}Ge(d,^{3}He)^{71}Ga$	$\geq$ 0.05	1.04	0.56	1.49
$^{74}Ge(d,^{3}He)^{73}Ga$	$\geq$ 0.04	1.12	0.23	1.24
$^{76}Ge(d,^{3}He)^{75}Ga$	0.15	1.24	0.23	1.82

Figure captions:

Figures 4.4a-b: Ground-state proton occupancies for nuclei using the Bhatt-Ahalpara (BA) and the fully renormalized Kuo-Brown (KB) effective interactions alongwith the experimental results. Experimental results are taken from reference nos. 43 and 44.

Figures 4.5a-b: Locations of SNT centroids of the target and the final nuclei. (a) theoretical (——) and experimental (----) centroids for stripping and pickup reactions on ^{68}Zn and ^{70}Ge targets respectively, (b) similar results for stripping reaction on ^{64}Zn and ^{66}Zn targets. Left half of each figure corresponds to BA interaction and right half corresponds to KB interaction; (i)stripping centroid for Zn target using bivariate gaussian approach, (ii) stripping centroid for Zn target using equation 32, (iii) experimental centroid for stripping reaction on Zn, (iv) experimental centroid for pickup reaction on Ge and (v) pickup centroid for Ge target using bivariate gaussian approach.

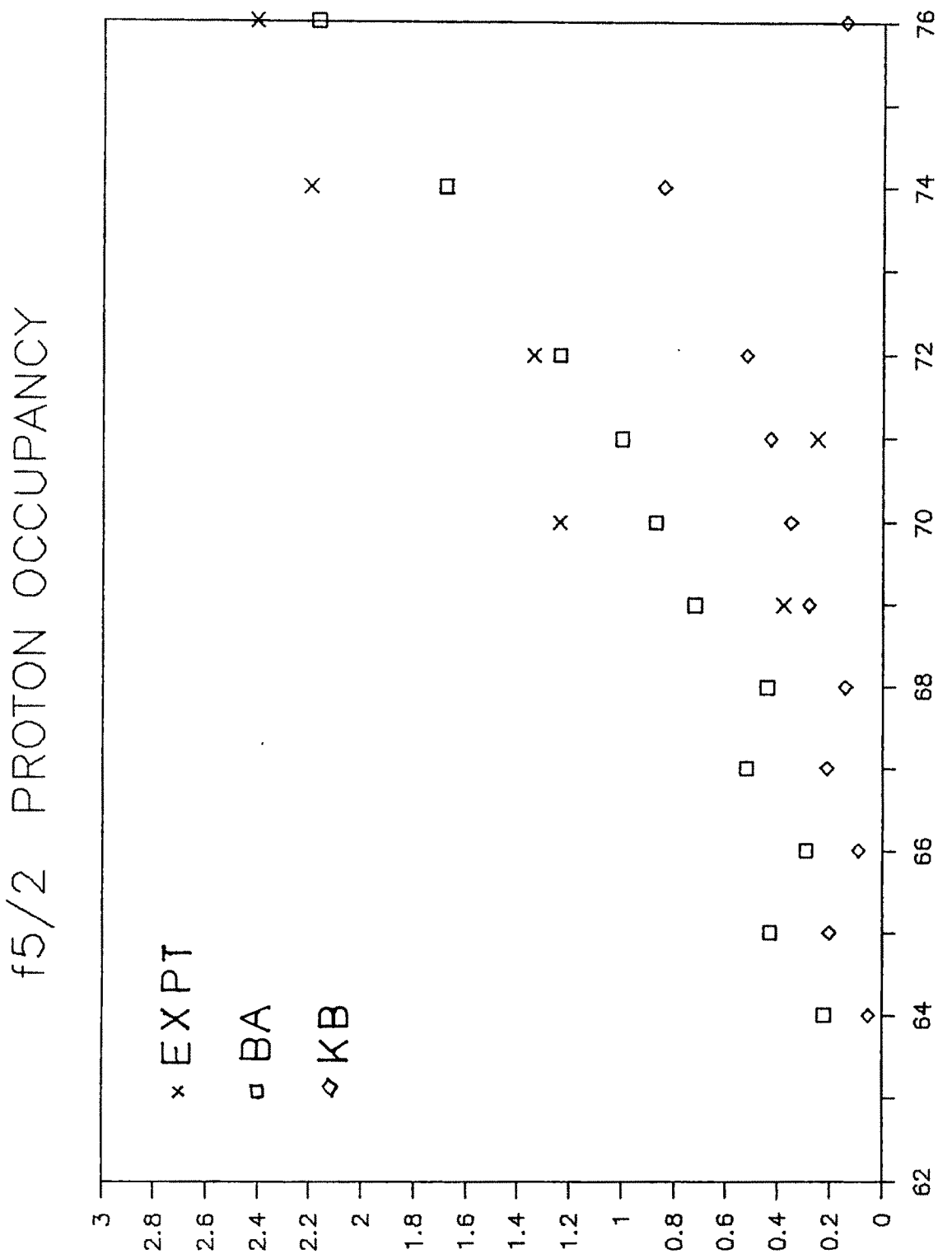
f5/2 PROTON OCCUPANCY
× EXPT
□ BA
◇ KB
MASS NUMBER
62
64
66
68
70
72
74
76
0
0.2
0.4
0.6
0.8
1
1.2
1.4
1.6
1.8
2
2.2
2.4
2.6
2.8
3

Fig. 4.4a

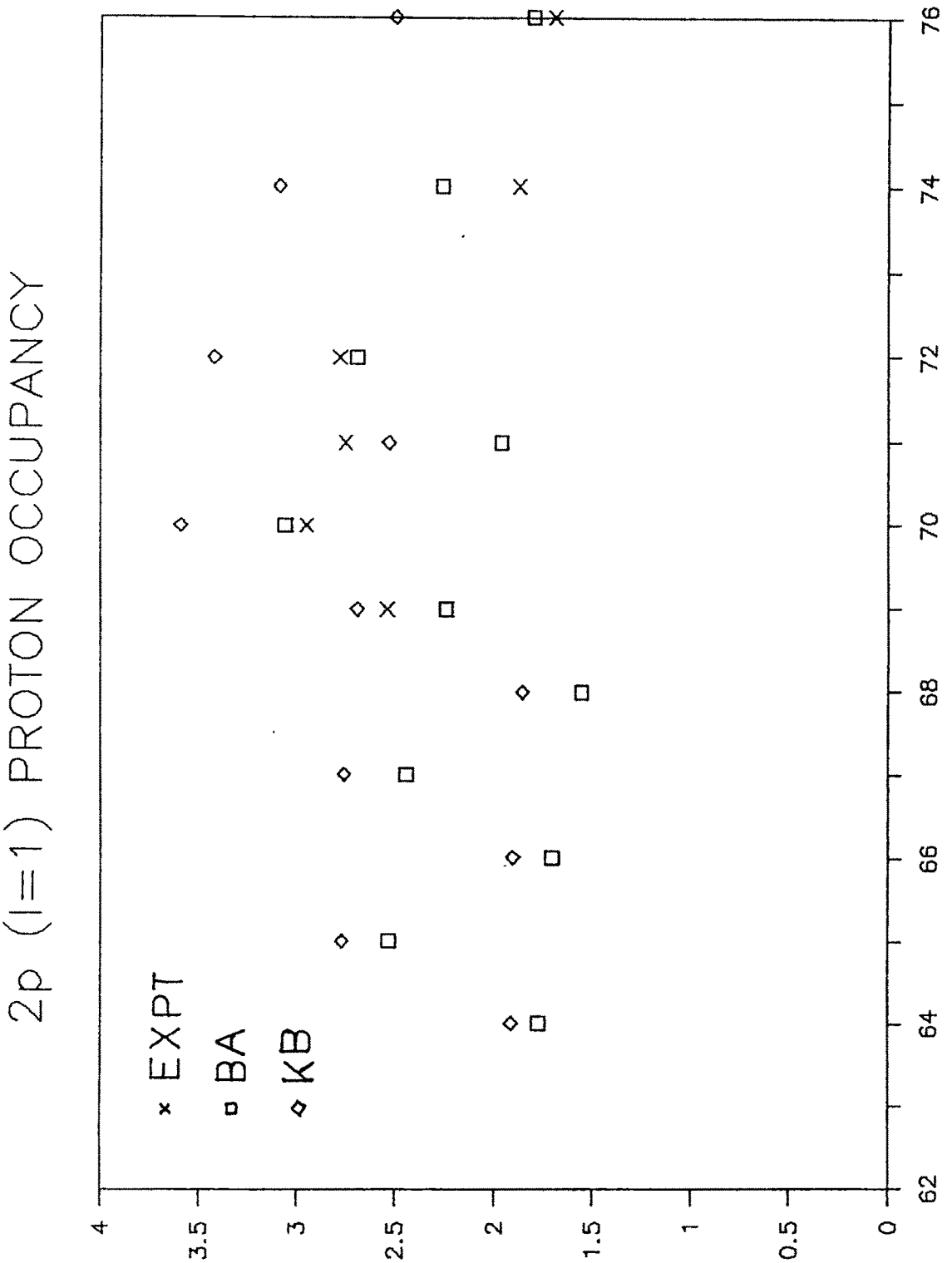
2p (I=1) PROTON OCCUPANCY
EXPT
BA
KB
4
3.5
3
2.5
2
1.5
1
0.5
0
62
64
66
68
70
72
74
76
MASS NUMBER

Fig. 4.4b

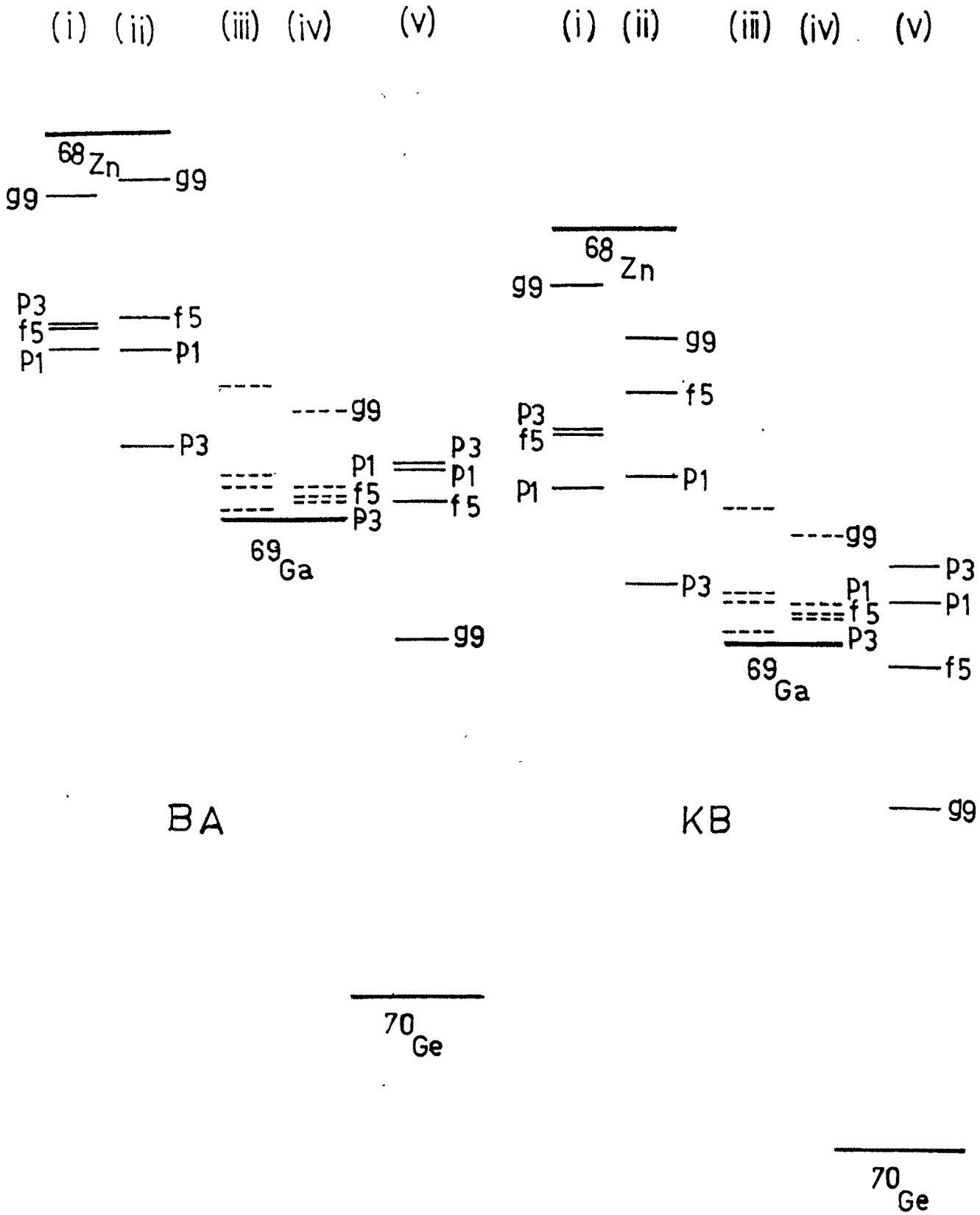
(i) (ii) (iii) (iv) (v)
68Zn
g9
g9
P3
f5
P1
f5
P1
P3
g9
P1
f5
P3
69Ga
P3
P1
f5
g9
BA
(i) (ii) (iii) (iv) (v)
68Zn
g9
g9
f5
P3
f5
P1
P1
P3
g9
P1
f5
P3
69Ga
P3
P1
f5
g9
KB
70Ge
70Ge

Fig. 4.5a

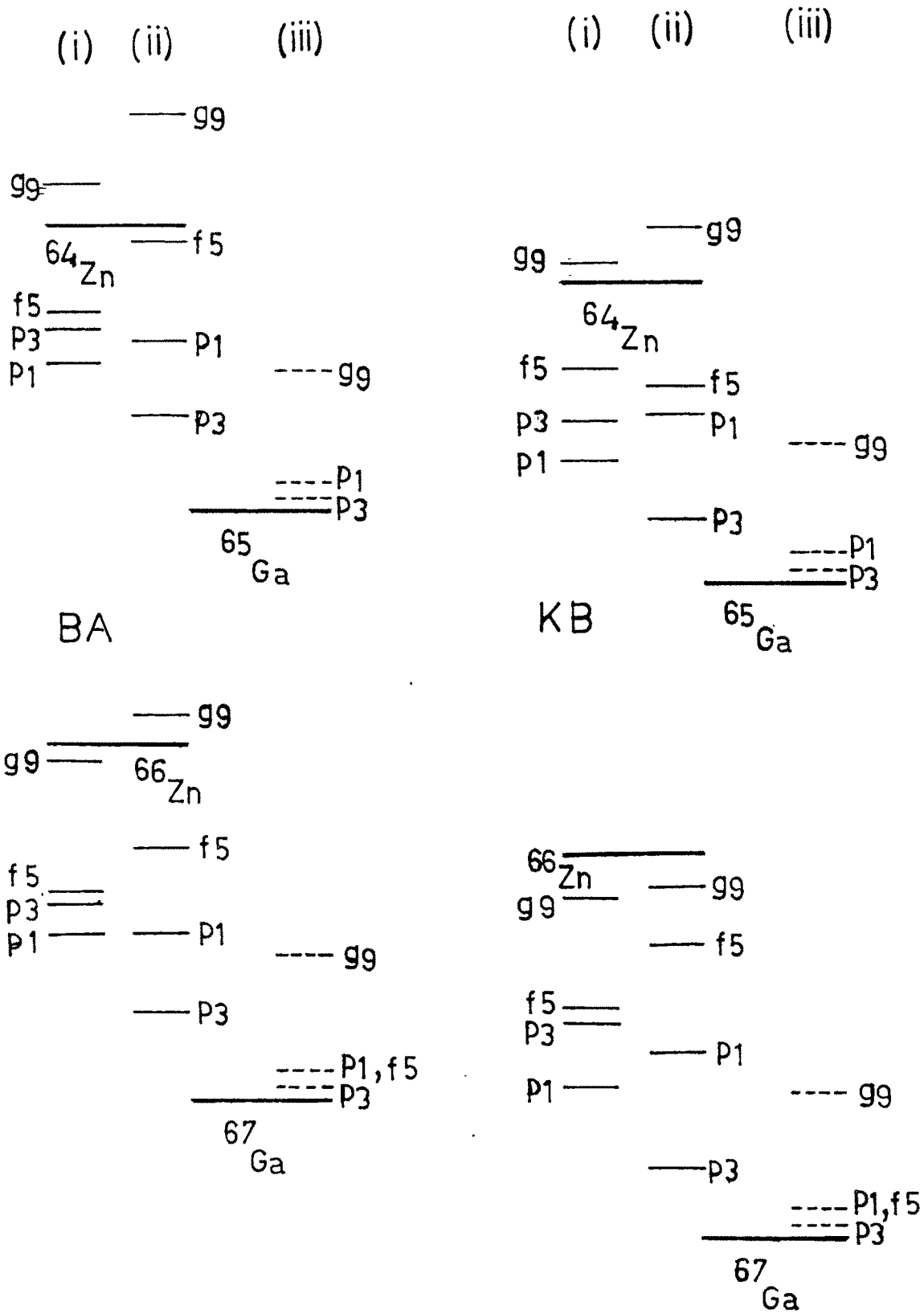

Fig. 4.5b

compared with the experimental results, $f_{5/2}$ proton occupancies for Ga isotopes are lower and nearer to the predictions of the KB interaction . For Ge isotopes, a sudden jump is observed in the experimental occupancies, particularly between ^{72}Ge and ^{74}Ge. This jump is at the expense of the $p_{3/2}$ orbit occupancy. This behaviour, particularly the increase in $f_{5/2}$ occupancy is well reproduced by the BA interaction and to a certain extent also by KB interaction. There is correspondingly a drop observed in occupancies of all the other orbits for different isotopes of a nucleus, this being the general trend for the BA interaction occupancies. From literature, we can infer that the sudden shift in experimental occupation from $p_{3/2}$ orbit to $f_{5/2}$ orbit could indicate a sharp structural change occurring between mass numbers A = 70-74. No such structural changes can be predicted from the theoretical results.

The proton addition strength centroid positions below the target nucleus are plotted in Figs.4.5a-b, for both theoretical and experimental values. No comparison can be made due to large uncertainities involved in the experimental data. Since one deals with higher excitation energies in the upper f-p shell, it turns out that at times more than half the strength is unresolved. The experimental centroids are calculated by taking into consideration only low energy excitation, and so correspond to the lower limit rather than the actual centroids for the different orbits. This is clear from Fig. 4.5a , where all experimental centroids lie below the theoretical predictions, and closer to the ground state level of the Ga nucleus. The experimental energy centroids observed in Ga as a result of both stripping and pickup reactions on Zn and Ge target nuclei lie close to each other.

This does not happen for theoretical predictions of centroids of pickup and stripping strengths. The experimental trend is partially reproduced by particle addition centroids. Particle removal centroid EMNS predicts a completely reverse trend. This is expected, due to the manner in which EP2 and EMNS are calculated. The centroids for both effective interactions follow exactly the same pattern, and are plotted side by side. Similar plots can be obtained for neutron centroids of particle removal and addition strengths. However, experimental results (which are given for only Zn isotopes) are extremely uncertain to be compared with the theoretical results.

Since no experimental data absorb the complete strength for any orbit in the case of both stripping and pickup reactions, it is difficult to estimate the experimental width for any SNT reaction with this data. Most of the experiments conducted display distribution of strengths upto maximum 2.5 to 3.0 MeV excitation energies. If we include unresolved strengths also, the region of spread of strength for both stripping and pickup reactions for 2p and $f_{5/2}$ orbits ranges from 1.5-2.5 MeV, which is also predicted by the theoretical widths. There is one major discrepancy that no spread is observed experimentally for $g_{9/2}$ orbit, for which a single sharp energy level carrying 90% of the total strength is seen. The theoretical results show a spread of 2 MeV even for the $g_{9/2}$ orbit, which is not seen experimentally.

C Summary

Single particle properties have been studied via sum-rules for a large number of nuclei lying in the 2s-1d shell, the f-p shell and the upper f-p-g shell, using the spectral distribution methods. All calculations are performed using configuration proton-neutron partitioning of space.

In the s-d shell, we have evaluated proton and neutron orbit occupancies using two standard interactions and compared these with the experimental values. Both the effective interactions, i.e. the PW interaction and Wildenthal's universal s-d interaction do quite well. The particle transfer centroids and widths have also been calculated and their positions with respect to ground states of targets and final nuclei have been displayed. It has been shown that the strength function when written as a sum of bivariate gaussians is a good approximation, to the extent that, the sum-rule quantities calculated using this approximation agree quite well with the polynomial expansion results. Apart from these, the occupancy dependent single particle energies have been evaluated and compared with the experimental values, where also a good agreement between the two is obtained.

For nuclei lying in the f-p shell region, we have calculated the effective single particle energies using known occupancy data of four effective interactions, namely the KB3p-1h, MWH, MWH2 and KB10. The experimental single particle energies are plotted alongwith those predicted by the four effective interactions. On the average, predictions of the KB3p-1h and the MWH2 interactions are closer to the experimental results than the others. Experimentally, a characteristic behaviour is observed for the $f_{7/2}$-$p_{3/2}$ energy gap. This gap shows a peak at magic number 28. This energy gap is therefore calculated for the four effective interactions. It is found that the MWH2 interaction gives a higher value of $f_{7/2}$-$p_{3/2}$ energy difference for every isotope having N = 28, and also for all isotopes of Fe(Z = 28). Other interactions are not consistent in this respect. From this point of view, the MWH2 can be said to prove better that the other effective interactions considered here.

It is usually observed, that a part of the experimental strength of some of the nuclei of the f-p shell spreads to the higher lying $g_{9/2}$ orbit. These nuclei can be treated as members of the upper f-p-g shell, and strengths can be normalized accordingly. Here, we use two effective interactions of the upper f-p-g shell to calculate ground state occupancies, centroids and widths of particle removal and addition strengths for few nuclei, including mainly isotopes of Zn, Ga and Ge. For this region, we have used constant configuration width approximation, in order to make computations feasible. It is seen that occupancies given by the Bhatt-Ahalpara effective interaction agree fairly well with the experimental values, for both protons and neutrons. The $f_{5/2}$ occupancies are slightly lower than the experimental occupancies, but compare much better than those given by the fully renormalized Kuo-Brown interaction. The experimental trend is reproduced by both the effective interactions. The centroids of both particle removal and addition strengths have also been compared with experimental results. Due to weak strength observed experimentally, the experimental energy centroids lie very low. The centroids (for different orbits) of the particle addition strength for both the effective interactions display the same order as that given by the experimental centroids. Also, it is found that, the magnitude of spread of strength experimentally for $p_{3/2}$, $f_{5/2}$ and $p_{1/2}$ orbits is comparable with the calculated widths of the SNT reactions.

As a comparative view of all the three shells, it can be said that results for the s-d shell compare better with experiments, than the f-p or f-p-g shell. One reason for this could be that both the effective interactions used in the s-d shell are known to give results nearly as good as those given by exact

calculations. Both of them also show nearly the same results. For the f-p and upper f-p-g shells, no effective interaction is known to work so well. The four interactions used in f-p shell clearly differ from each other a lot with respect to their occupancy or energy predictions. Other reasons for discrepancies observed between experimental and theoretical results for f-p and upper f-p-g shell could be: less data due to scarcity of experiments conducted, absence of a considerable percentage of strength available for sum-rule analysis, and so on. Also, the spread of strength is reduced (theoretically) from s-d shell to upper f-p-g shell. This could imply overlapping of strengths or unresolved strength, experimentally.